bioRxiv preprint doi: https://doi.org/10.1101/2023.04.21.537482; this version posted April 23, 2023. The copyright holder for this preprint (which was not certified by peer review) is the author/funder, who has granted bioRxiv a license to display the preprint in perpetuity. It is made available under aCC-BY-NC-ND 4.0 International license.

Learning from the expert: studying *Salicornia* to understand salinity tolerance

Octavio R. Salazar[1,2,3], Ke Chen[4], Vanessa J. Melino[1,2], Muppala P. Reddy[1,2], Eva Hřibová[5], Jana Čížková[5], Denisa Beránková[5], Manuel Aranda[1,3], Lukasz Jaremko[1], Mariusz Jaremko[1], Nina V. Fedoroff[6], Mark Tester[1,2#] & Sandra M. Schmöckel[7]

[1] Biological and Environmental Sciences & Engineering Division (BESE), King Abdullah University of Science and Technology (KAUST), Thuwal, 23955-6900, Kingdom of Saudi Arabia

[2] Center for Desert Agriculture, King Abdullah University of Science and Technology (KAUST), Thuwal, 23955-6900, Kingdom of Saudi Arabia

[3] Red Sea Research Center, King Abdullah University of Science and Technology (KAUST), Thuwal, 23955-6900, Kingdom of Saudi Arabia

[4] Rice Research Institute, Guangdong Academy of Agricultural Sciences, Guangzhou, 510640, China

[5] Institute of Experimental Botany of the Czech Academy of Sciences, Centre of Plant Structural and Functional Genomics, Šlechtitelů 31, 77900 Olomouc, Czech Republic

[6] Department of Biology, Penn State University, University Park, PA 16801, United States

[7] Department Physiology of Yield Stability, Institute of Crop Science, University of Hohenheim, Fruwirthstr. 21, 70599 Stuttgart, Germany

[#] Corresponding author: Mark Tester

bioRxiv preprint doi: https://doi.org/10.1101/2023.04.21.537482; this version posted April 23, 2023. The copyright holder for this preprint (which was not certified by peer review) is the author/funder, who has granted bioRxiv a license to display the preprint in perpetuity. It is made available under aCC-BY-NC-ND 4.0 International license.

Abstract

Salinity remains a major inhibitor of crop production in irrigated and marginal lands. The identification of genes involved in salinity tolerance has been predominantly limited to model plants and crop species. However, plants naturally adapted to highly saline environments can provide key insights into mechanisms of salinity tolerance. Plants of the genus *Salicornia* grow in coastal salt marshes, and their growth is even stimulated by NaCl – much can be learnt from them. We generated genome sequences of two *Salicornia* species and studied the transcriptomic and proteomic responses of *Salicornia bigelovii* to NaCl. Through the generation of subcellular membrane proteomes, we found that SbiSOS1, a homolog of the well-known SALT-OVERLY-SENSITIVE 1 (SOS1) protein, appears to localize to the tonoplast, where it could be involved in mediating Na^+ translocation into the vacuole to prevent toxicity in the cytosol. We identified 11 proteins of interest which, when expressed in yeast, altered salinity tolerance. One of these proteins, SbiSALTY, substantially improves yeast growth on saline media. Structural characterization using NMR showed it to be an intrinsically disordered protein and to localize to the endoplasmic reticulum *in planta*, where it could interact with ribosomes and RNA, potentially stabilizing or protecting them during salt stress. The study and understanding of the molecular mechanisms providing high salinity tolerance in *S. bigelovii* is likely to provide significant insights for improving salinity tolerance of crop plants.

bioRxiv preprint doi: https://doi.org/10.1101/2023.04.21.537482; this version posted April 23, 2023. The copyright holder for this preprint (which was not certified by peer review) is the author/funder, who has granted bioRxiv a license to display the preprint in perpetuity. It is made available under aCC-BY-NC-ND 4.0 International license.

Main

Salinity is one of the major factors limiting crop productivity, with most crops being relatively salt sensitive and significantly affected when exposed to NaCl in the range of 50 to 200 mM[1]. Currently, at least 20% of irrigated lands are affected by salinity[2] and this is increasing[3,4]. With the world's population projected to grow from 7.7 to 9.7 billion people by 2050[5], the demand for increased agricultural production will likely require expanding crop production on marginal land, including saline soils. Studies in salinity tolerance have primarily focused on plants that grow at low concentrations of salt, which includes all major crops. However, plants that thrive in highly saline environments have the potential to be valuable in the development of salt tolerant crops, as they already possess adaptations that allow them to thrive in saline environments.

The genus *Salicornia* belongs to the subfamily Salicornioideae in the Amaranthaceae family and plants of this genus grow in coastal salt marshes and inland salt lakes throughout the world[6]. They are amongst the most salt tolerant of all plant species and can thrive in environments with salinities even higher than seawater[7,8]. Notably, *Salicornia* plants can accumulate high concentrations of Na^+ in their photosynthetically active succulent shoots while avoiding ion toxicity[7,9,10], suggesting highly efficient ion compartmentalization processes in cells through the action of specialized transporters[11-14]. Moreover, *Salicornia* growth is promoted by the addition of NaCl[10,15-17], making it a particularly interesting genus for the study of salinity tolerance.

In this study, we generated draft genome sequences for two Salicornioideae species: *Salicornia bigelovii*, endemic to Mexico and the United States; and *Salicornia europaea*, endemic to Europe, Northern Africa, the Middle East, and Central Asia. We

bioRxiv preprint doi: https://doi.org/10.1101/2023.04.21.537482; this version posted April 23, 2023. The copyright holder for this preprint (which was not certified by peer review) is the author/funder, who has granted bioRxiv a license to display the preprint in perpetuity. It is made available under aCC-BY-NC-ND 4.0 International license.

then focused on *S. bigelovii* and investigated its phenotypic, transcriptomic, and proteomic responses to different concentrations of NaCl, generating organellar membrane proteomes to enable allocation of membrane proteins to particular organelles. The protein SALT-OVERLY-SENSITIVE 1 (SOS1) unexpectedly appears to be localized to the vacuolar membrane, suggesting its neo-localization in *S. bigelovii*. Based on the transcriptomic and proteomic responses, we selected 45 candidate genes likely to contribute to salinity tolerance in *S. bigelovii* and found 11 altering salinity tolerance in a yeast expression system. We also further investigated a protein we named SALTY, which greatly improved salinity tolerance when expressed in yeast. Using nuclear magnetic resonance (NMR), SALTY was found to be an intrinsically disordered protein. This protein was localized to the endoplasmic reticulum (ER) where it is likely to interact with ribosomes and RNA.

Results

NaCl stimulates growth of *S. bigelovii*

We analyzed the phenotypic responses of *S. bigelovii* to NaCl by treating 5-week-old plants with 0, 50, 200, and 600 mM NaCl. After 1 week, plants treated with NaCl were taller than plants treated with 0 mM NaCl, and plants treated with 200 and 600 mM NaCl developed lateral branches (Fig. 1a,b). The beneficial effects of NaCl became increasingly apparent with time, and 6 weeks after treatment, all plants supplemented with NaCl were significantly taller and displayed a lighter green hue (Fig. 1c,d). Plants treated with 600 mM NaCl were shorter than those treated with 50 or 200 mM NaCl, but

bioRxiv preprint doi: https://doi.org/10.1101/2023.04.21.537482; this version posted April 23, 2023. The copyright holder for this preprint (which was not certified by peer review) is the author/funder, who has granted bioRxiv a license to display the preprint in perpetuity. It is made available under aCC-BY-NC-ND 4.0 International license.

had thicker shoots (Fig. 1e,f), which is in agreement with previous studies reporting 200 mM NaCl as the optimum concentration for *S. bigelovii* growth[10,15-18].

S. bigelovii accumulates large amounts of Na^+ and Cl^- in its shoots

High concentrations of NaCl are usually detrimental to plants, as ion accumulation in shoots may lead to cell toxicity and premature senescence[1,19,20]. In plant cells, K^+ is usually at least 10 times more abundant than Na^+, with cells experiencing Na^+ toxicity when the Na^+/K^+ is altered in favor of Na^+ [21], as Na^+ and K^+ are thought to compete for functionally important binding sites inside the cell[22-24].

Na^+ and Cl^- concentrations increased in shoots and roots with increasing NaCl treatment (Fig. 1g,h). We found Na^+ and Cl^- concentrations in excess of 750 mM in the shoots and 400 mM in the roots of *S. bigelovii* treated with 600 mM NaCl, which accounted for 60% of shoot and 10% of root dry mass (Supplementary Fig. 1). K^+ concentrations decreased with increasing NaCl treatment (Fig. 1i) and Na^+/K^+ was greater than 1 in shoots in all treatments**,** being over 20 times greater in plants treated with 600 mM NaCl (Supplementary Fig. 1). In roots, Na^+ concentrations were less than two-fold higher than K^+ at 600 mM NaCl. Shoot sap osmolality increased with NaCl treatment (Supplementary Data Fig. 1). Water content was higher in shoots compared with roots and increased with NaCl treatment (Fig. 1j). It was positively correlated with both Na^+ and Cl^- and negatively correlated with K^+ (Supplementary Data Fig. 2), suggesting that Na^+ and Cl^- could be used as osmolytes to facilitate water retention in the shoots[25].

bioRxiv preprint doi: https://doi.org/10.1101/2023.04.21.537482; this version posted April 23, 2023. The copyright holder for this preprint (which was not certified by peer review) is the author/funder, who has granted bioRxiv a license to display the preprint in perpetuity. It is made available under aCC-BY-NC-ND 4.0 International license.

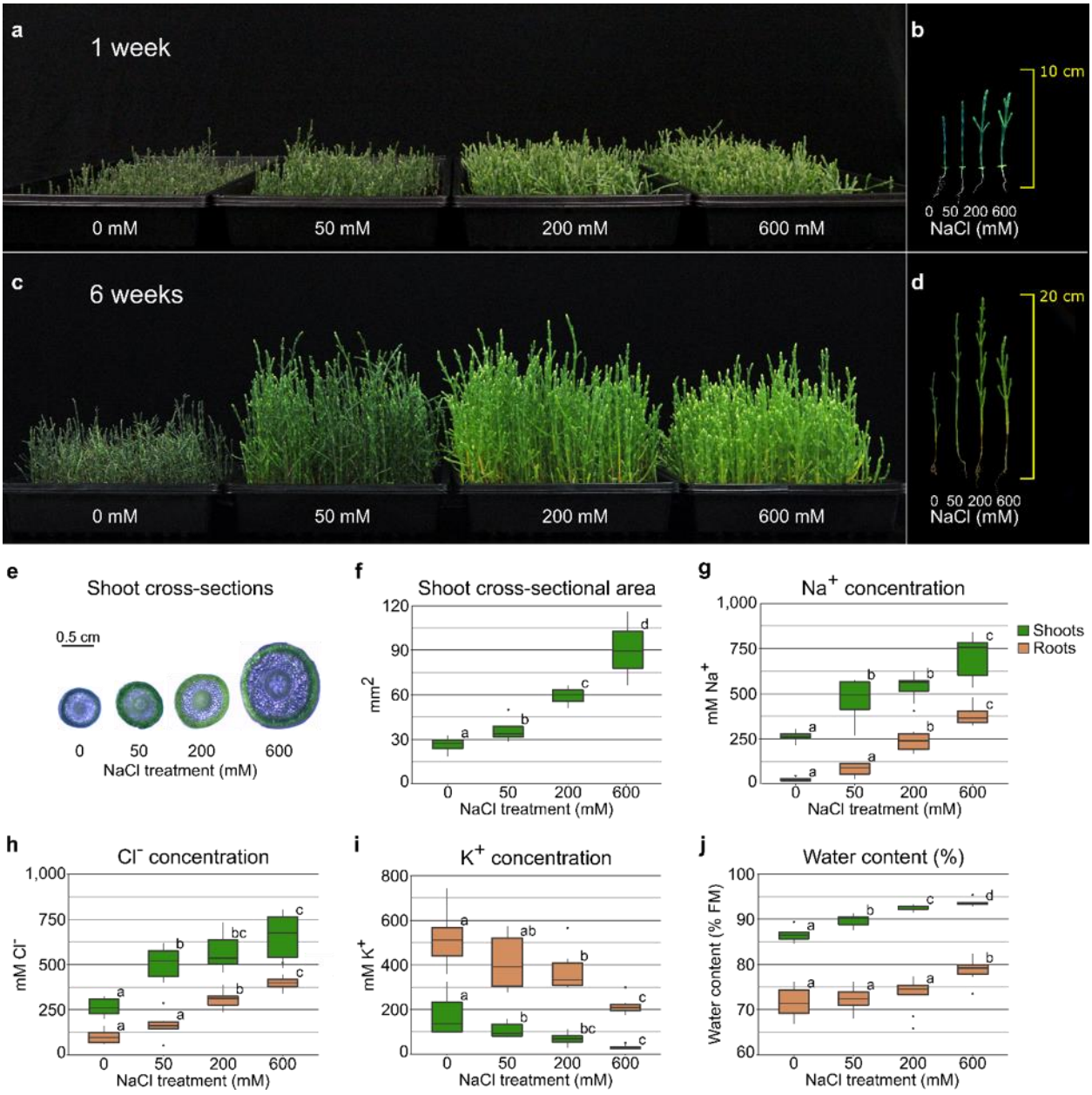

Figure 1. *S. bigelovii* growth and ion accumulation under different salinities. Plants were grown for 5 weeks prior to the addition of 0, 50, 200, or 600 mM NaCl. **a,** Plants 1 week after treatment. **b,** Length of individual plants 1 week after treatment. **c,** Plants 6 weeks after treatment. **d,** Length of individual plants 6 weeks after treatment. **e,** Shoot cross-sections. **f,** Shoot cross-sectional area **g,** Na^+ concentration in shoots and roots. **h,** Cl^-

bioRxiv preprint doi: https://doi.org/10.1101/2023.04.21.537482; this version posted April 23, 2023. The copyright holder for this preprint (which was not certified by peer review) is the author/funder, who has granted bioRxiv a license to display the preprint in perpetuity. It is made available under aCC-BY-NC-ND 4.0 International license.

concentration in shoots and roots. **i,** K^+ concentration in shoots and roots. **j,** Water content in shoots and roots. n = 9, mean differences were compared within each tissue and the FDR was controlled with the Benjamini-Hochberg procedure at an $\alpha = 0.05$, significant differences are indicated as different letters.

Genome sequencing and assembly

To gain insight into the molecular mechanisms driving the outstanding salt tolerance of *Salicornia*, we first generated genome assemblies for two *Salicornia* species: *S. bigelovii,* an autotetraploid (2n = 4x = 36)[6], and *S. europaea*, a diploid (2n = 2x = 18)[6,26]. Here we used PacBio HiFi sequencing to generate near chromosome-scale genome assemblies, resulting in haploid genome assemblies of 2,026 and 517 Mb for *S. bigelovii* and *S. europaea*, respectively (Supplementary Table 1). These assemblies encompassed >99% of the genome in 33 contigs for *S. bigelovii* and 20 for *S. europaea*. The genome assemblies were in line with flow cytometry-based genome size estimates and showed high assembly completeness[27,28] (Supplementary Figs. 3 and 4). *S. europaea* flow cytometry values were similar to what has been reported for diploid *Salicornia* in the Gulf of Trieste[29], yet interestingly, *S. bigelovii* shows a larger genome of almost double the size of previously reported tetraploid *Salicornia*. One of the potential causes for this could be the increased percentage of repetitive elements in the genome of *S. bigelovii* (Supplementary Table 1), but further investigation is required. The genomes were predicted to contain 63,843 and 28,794 genes for *S. bigelovii* and *S. europaea*, respectively. The predicted proteins were annotated against Swiss-Prot, TrEMBL[30], NCBI NR[31], MapMan[32,33], and KEGG[34] databases (Supplementary Data

bioRxiv preprint doi: https://doi.org/10.1101/2023.04.21.537482; this version posted April 23, 2023. The copyright holder for this preprint (which was not certified by peer review) is the author/funder, who has granted bioRxiv a license to display the preprint in perpetuity. It is made available under aCC-BY-NC-ND 4.0 International license.

Files 1 and 2). The completeness of the gene prediction was assessed with BUSCO[35], resulting in completeness scores of 96.3% and 95.3% for *S. bigelovii* and *S. europaea*, respectively (Supplementary Table 1).

Gene orthology analysis

To explore possible genetic adaptations of *Salicornia* to salinity we identified groups of orthologous proteins across representative genomes of five plant families (Brassicaceae, Amaranthaceae, Fabaceae, Solanaceae, and Poaceae) with OrthoMCL[36], aiming to identify groups of proteins specific to different plant clades. A total of 38,356 orthogroups were identified, composed of 355,771 proteins (Supplementary Data File 3). Phylogenetic reconstruction based on 1,377 orthologs, resulted in a resolved phylogeny by family with the genus *Salicornia* forming a subclade within the family Amaranthaceae (Supplementary Fig. 5). A total of 9,470 orthogroups were shared across all families (Fig. 2a), and gene ontology (GO)[37,38] enrichment analyses of unique orthogroups revealed enrichments specific to each family (Supplementary Data File 3). Orthogroups unique and present in all Amaranthaceae, were enriched in GO terms such as ‘response to reactive oxygen species’, ‘positive regulation of sodium ion transport’, ‘clustering of voltage-gated sodium channels’, and ‘positive regulation of protein targeting to membrane’ (Supplementary Data File 3), which could in part explain the high salt tolerance of plants in this family.

When looking at orthogroups within the Amaranthaceae, the majority of the orthogroups were found in all species, sharing 11,350 orthogroups (Fig. 2b). GO enrichment analysis of unique orthogroups in *Salicornia* species identified enrichment of

bioRxiv preprint doi: https://doi.org/10.1101/2023.04.21.537482; this version posted April 23, 2023. The copyright holder for this preprint (which was not certified by peer review) is the author/funder, who has granted bioRxiv a license to display the preprint in perpetuity. It is made available under aCC-BY-NC-ND 4.0 International license.

terms related to light, in the form of 'response to UV-A', 'response to far red light', and 'response to high light intensity'; to 'ion binding', in the form of zinc and manganese; to toxin production, in the form of 'toxin catabolic and metabolic processes'; and to 'mechanically gated ion channel', particularly in the form of calcium channels. These calcium channels could be involved in calcium wave signaling during NaCl stress[39-41]. Nevertheless, no orthogroup was enriched for Na^+ transport.

We then looked at possible expansions of sodium/proton exchanger (NHX) proteins of the cation/proton antiporter (CPA) family, which are commonly associated with salt tolerance. Phylogenetic reconstruction of NHX proteins resulted in clustering by type and family (Fig. 2c and Supplementary Data File 4). We identified 6 NHX proteins in *S. bigelovii* and *S. europaea*, of which 4 resembled the *Arabidopsis thaliana* vacuolar NHX1-4[42-44], one resembled the endosomal NHX6[45], and one the plasma membrane NHX7, also known as SALT-OVERLY-SENSITIVE 1 (SOS1)[46] (Fig. 2c). Both contained only one endosomal NHX protein and no homolog for the Li^+/H^+ antiporter NHX8[47] was identified in either *Salicornia* genome, similarly to what has been observed in sugar beet[48], another Amaranthaceae. Furthermore, proteins resembling NHX8 from families other than Brassicaceae, are small in size, appear to be truncated, and are usually localized next to an ORF coding for a complementary protein, that when combined, resemble SOS1. Further inspection would be required to identify if this is the result of the degeneration of a previous duplication event, or if it is an artefact of gene prediction. These results show no *NHX* gene expansion in *Salicornia*, indicating that its outstanding salt tolerance does not come from an increased repertoire of NHX proteins. We then looked at gene expansions in *Salicornia*, defined as having at least twice the number of

bioRxiv preprint doi: https://doi.org/10.1101/2023.04.21.537482; this version posted April 23, 2023. The copyright holder for this preprint (which was not certified by peer review) is the author/funder, who has granted bioRxiv a license to display the preprint in perpetuity. It is made available under aCC-BY-NC-ND 4.0 International license.

proteins in *S. bigelovii* and *S. europaea* when compared to any other species within the orthogroup. GO enrichment analysis of these proteins revealed enrichments in terms related to transposable elements and iron transport, but no term was related to sodium transport (Supplementary Data File 3). All together, these results suggest that *Salicornia* could have a different repertoire of currently unknown genes involved in salinity tolerance or that it has fine-tuned the same genes found in other species to cope with extremely saline environments.

bioRxiv preprint doi: https://doi.org/10.1101/2023.04.21.537482; this version posted April 23, 2023. The copyright holder for this preprint (which was not certified by peer review) is the author/funder, who has granted bioRxiv a license to display the preprint in perpetuity. It is made available under aCC-BY-NC-ND 4.0 International license.

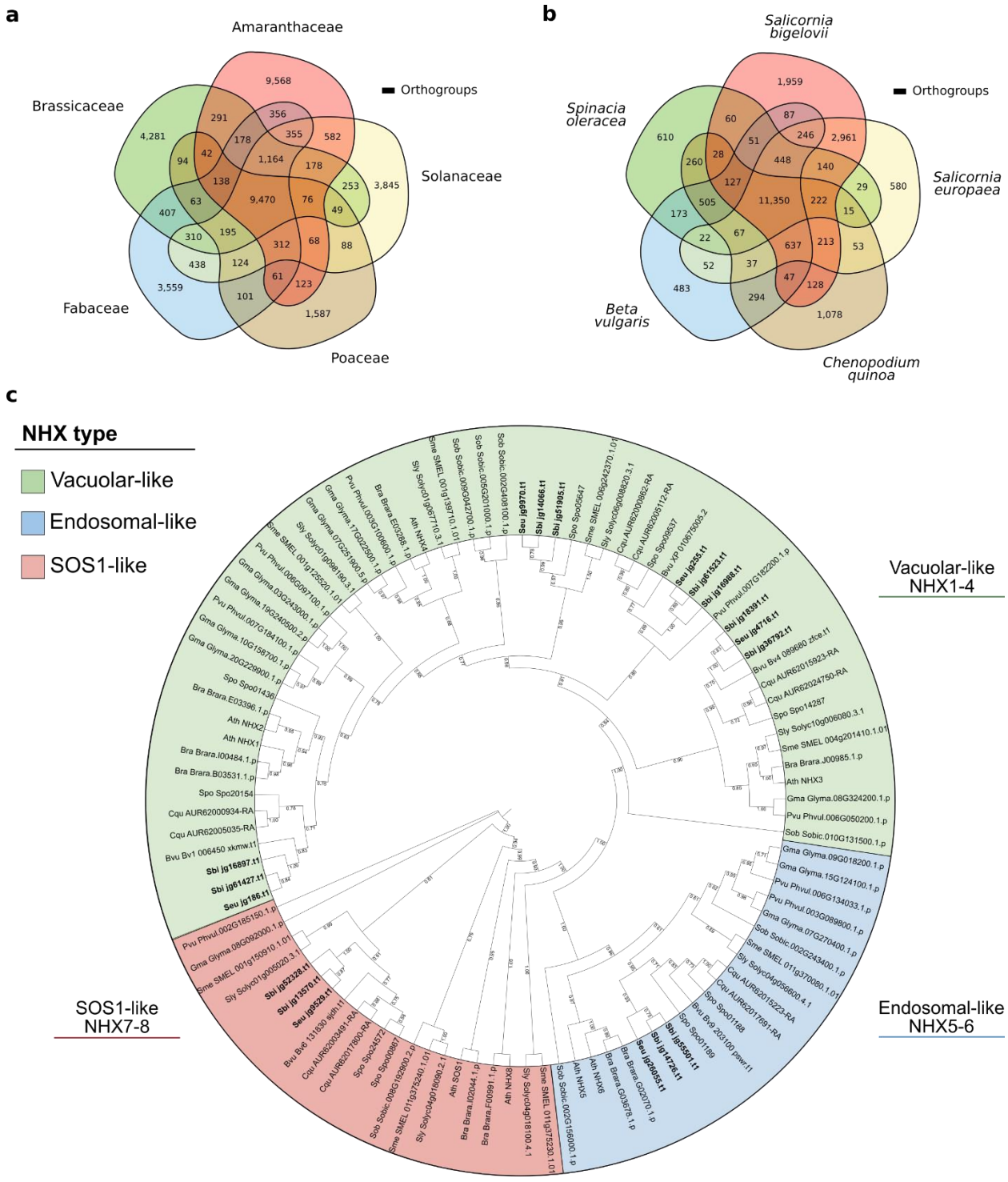

Figure 2. Conservation of orthologous proteins across families and species. **a,** Number of orthogroups shared across the families Brassicaceae (*Arabidopsis thaliana*, *Brassica*

bioRxiv preprint doi: https://doi.org/10.1101/2023.04.21.537482; this version posted April 23, 2023. The copyright holder for this preprint (which was not certified by peer review) is the author/funder, who has granted bioRxiv a license to display the preprint in perpetuity. It is made available under aCC-BY-NC-ND 4.0 International license.

rapa), Amaranthaceae (*Beta vulgaris*, *Chenopodium quinoa*, *S. bigelovii*, *S. europaea*, *Spinacia oleracea*), Fabaceae (*Glycine max*, *Phaseolus vulgaris*), Solanaceae (*Solanum lycopersicum*, *Solanum melongena*), and Poaceae (*Sorghum bicolor*). **b,** Number of orthogroups shared across the Amaranthaceae species: *Beta vulgaris*, *Chenopodium quinoa*, *S. bigelovii*, *S. europaea*, and *Spinacia oleracea*. **c,** Phylogenetic reconstruction of NHX proteins. In bold, *Salicornia* proteins. The phylogenetic tree was generated with RAxML-NG[49], values at branching nodes represent transfer bootstrap expectation (TBE)[50] values based on 1,000 replicates.

NaCl induces expression of genes associated with growth

To gain insights into the responses of *S. bigelovii* to NaCl, we studied the transcriptomic responses in shoots of plants exposed to 0, 50, 200, and 600 mM NaCl for 1 and 6 weeks. We identified 11,799 differentially expressed genes between at least two treatments (Fig. 3a, Supplementary Table 2, Supplementary Data File 4). Plants that were not treated with NaCl clustered together regardless of their age, while plants treated with NaCl clustered according to their age and treatment (Fig. 3a). This could be caused by the limited growth that plants displayed without the addition of NaCl and by the developmental responses that occurred upon NaCl treatment (Fig. 1). Plants treated with 600 mM NaCl for 1 week clustered separately from any time point or treatment and had the highest number of differentially expressed genes. This suggests a shock response to the high concentration of NaCl, as 6 weeks after treatment, their gene expression became similar to those treated with 50 and 200 mM NaCl, indicating that plants had adapted to the high concentration of NaCl (Fig. 3a).

bioRxiv preprint doi: https://doi.org/10.1101/2023.04.21.537482; this version posted April 23, 2023. The copyright holder for this preprint (which was not certified by peer review) is the author/funder, who has granted bioRxiv a license to display the preprint in perpetuity. It is made available under aCC-BY-NC-ND 4.0 International license.

GO enrichment analysis of genes upregulated in plants treated with NaCl revealed enrichment in terms related to growth, such as 'carbohydrate biosynthetic and metabolic processes', 'cell wall biogenesis and modification', 'regulation of cell size', and 'water transport' (Fig. 3b and Supplementary Data File 5). This is in agreement with the increased growth, cell size, and water content observed in *S. bigelovii* plants upon the addition of salt (Fig. 1). Conversely, plants grown in the absence of NaCl had enriched terms such as 'response to starvation', 'response to stress', 'response to nutrient levels', 'iron and nitrate transport', 'starch metabolic process', and 'lipid, terpenoid and oxylipin biosynthetic processes', indicating that plants grown without salt were under stress and suffered nutritional imbalance (Fig. 3c and Supplementary Data File 5). MapMan[32,33] pathway analysis revealed similar results (Supplementary Tables 3 and 4), but also showed an enrichment in the downregulation of genes coding for receptor proteins with domain of unknown function 26 (DUF26). This downregulation was greatly overrepresented in plants treated with 600 mM NaCl for 1 week. Downregulation of the DUF26 protein, OsRMC, in rice increased survival of rice plants when exposed to severe NaCl treatments[51]. The increased downregulation of DUF26 proteins in *S. bigelovii* when exposed to high concentrations of NaCl could have a similar effect as in rice, increasing survival in high salinity.

We then looked at the expression of genes encoding transporter proteins commonly associated with salinity tolerance and found contrasting gene expression profiles (Fig. 3b-d). *SOS1* was upregulated in plants treated with NaCl, the high-affinity potassium transporter (*HKT1*)[52,53] expression was downregulated upon NaCl treatment, and *NHXs* gene expression remained constant throughout treatments (Supplementary

bioRxiv preprint doi: https://doi.org/10.1101/2023.04.21.537482; this version posted April 23, 2023. The copyright holder for this preprint (which was not certified by peer review) is the author/funder, who has granted bioRxiv a license to display the preprint in perpetuity. It is made available under aCC-BY-NC-ND 4.0 International license.

Data File 4). Previous studies in *Salicornia dolichostachya,* based on quantitative Reverse Transcription (qRT)-PCR, suggested *HKT1* to be absent from *Salicornia*[54]. However, we found *HKT1* to be present in both *Salicornia* species.

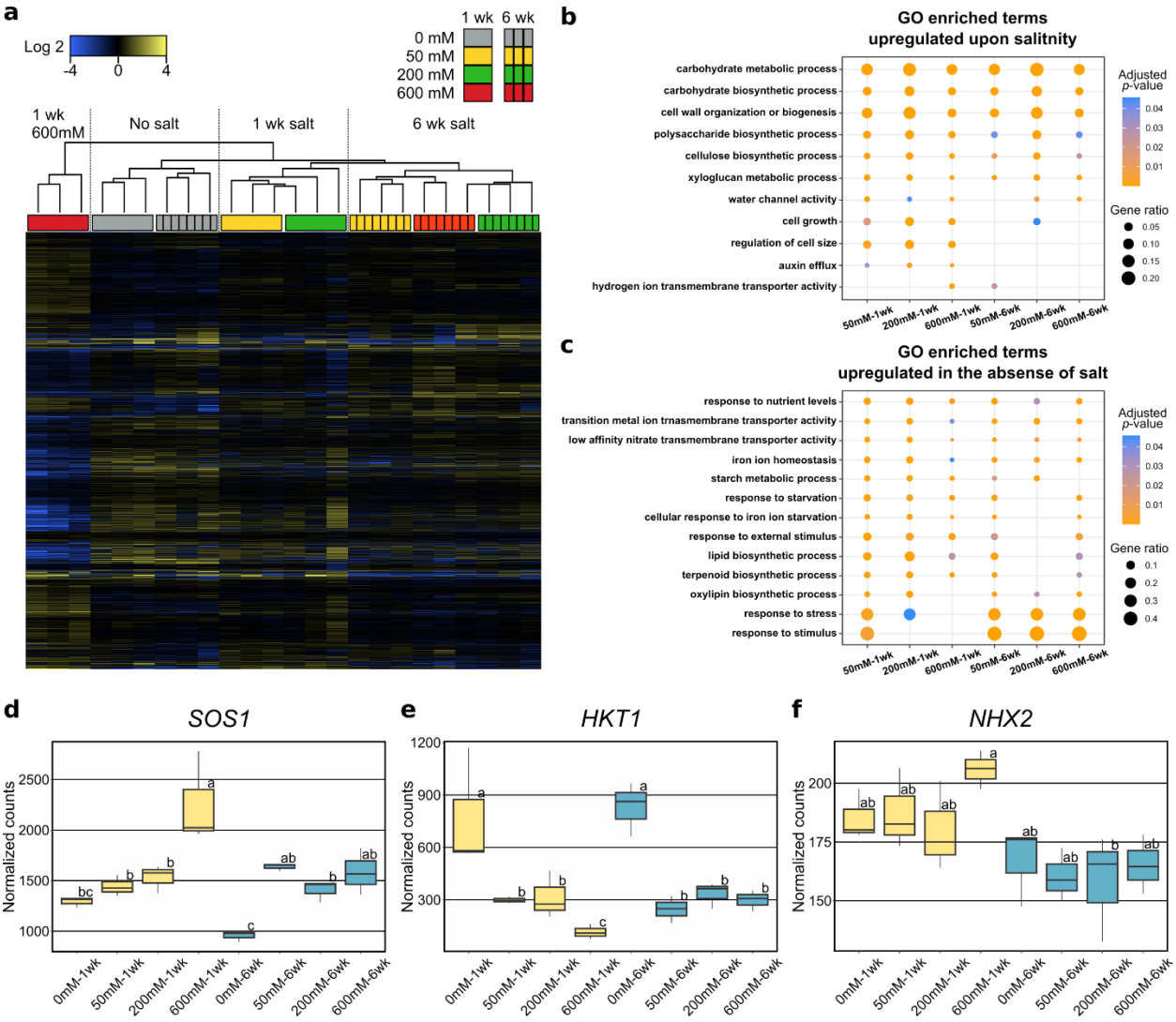

Figure 3. *S. bigelovii* transcriptional responses to NaCl. **a,** Hierarchical clustering of differentially expressed genes in shoots of *S. bigelovii* plants treated with 0, 50, 200, and 600 mM NaCl for 1 and 6 weeks. **b-c,** Representative GO enriched terms relative to 0mM NaCl treated plants. **b,** upregulated upon the addition of NaCl, **c,** upregulated in

bioRxiv preprint doi: https://doi.org/10.1101/2023.04.21.537482; this version posted April 23, 2023. The copyright holder for this preprint (which was not certified by peer review) is the author/funder, who has granted bioRxiv a license to display the preprint in perpetuity. It is made available under aCC-BY-NC-ND 4.0 International license.

0mM NaCl treated plants. **d-f,** Gene expression of proteins commonly associated with Na^+ transport. Yellow, plants treated for 1 week; Blue, plants treated for 6 weeks. **d,** *SOS1*, **e,** *HKT1*, **f,** *NHX2*.

S. bigelovii organellar membrane proteome

We hypothesized that specific ion transporters must play key roles in preventing ion toxicity in *S. bigelovii* cells, extruding Na^+ from the cytosol and compartmentalizing it in the vacuole. Proteomic analyses of specific membrane systems are possible as membranes from different organelles have different densities, allowing for their separation through ultracentrifugation[55,56] (Supplementary Fig. 6). The separation does not result in pure isolates, but in fractions enriched with membranes from specific organelles[57,58]. We isolated membrane-enriched fractions from shoots of *S. bigelovii* plants treated with 0, 50, 200, and 600 mM NaCl for 6 weeks, resulting in 12 different density fractions from a continuous sucrose gradient covering a specific gravity range, from 1.08 - 1.19 relative to water, and a maximum variation of 0.8% sucrose or 0.003 specific gravity within fractions (Supplementary Figs. 6 and 7).

Membrane proteins were digested using the gel-free filter-aided sample preparation protocol (FASP)[59], resulting in the identification of more than 1,500 protein clusters per treatment (Table 1) and a total of 2,118 unique protein clusters. Markers from 5 different organelles were identified based on previous proteomic studies in Arabidopsis[57,60-64].

bioRxiv preprint doi: https://doi.org/10.1101/2023.04.21.537482; this version posted April 23, 2023. The copyright holder for this preprint (which was not certified by peer review) is the author/funder, who has granted bioRxiv a license to display the preprint in perpetuity. It is made available under aCC-BY-NC-ND 4.0 International license.

Table 1. Total number of proteins identified and number of marker proteins per organelle for *S. bigelovii* membrane preparations from plants treated with 0, 50, 200, or 600 mM NaCl.

Marker type/NaCl	0 mM	50 mM	200 mM	600 mM
Endoplasmic reticulum	18	18	20	17
Mitochondrion	35	35	36	35
Plasma membrane	22	21	21	21
Chloroplast	30	23	32	25
Tonoplast	18	17	18	15
Total markers	**123**	**114**	**127**	**113**
Unallocated proteins	1,535	1,462	1,461	1,512
Total proteins	1,658	1,576	1,588	1,625

Organellar membrane profiles were generated by assessing the relative abundance of marker proteins at the different density fractions with pRoloc[65-70]. To validate the *in silico* organellar profiles generated with pRoloc, western blots were carried out across the 12 different density fractions against marker proteins for the thylakoid (PsbA-D1), plasma membrane (H^+-ATPase) and tonoplast (V-ATPase) (Fig. 4a, Supplementary Fig. 8). *In silico* organellar protein profiles coincided with the results obtained from western blots (Fig. 4a,b), indicating a good organelle profile accuracy of our *in silico* profiles. To allocate a subcellular localization to the unclassified proteins, their relative abundances were compared against organellar profiles across the 12 different density fractions (Fig. 4c and Supplementary Data File 6). Due to similarities in their densities, separation between the plasma membrane and endoplasmic reticulum (ER), and between the chloroplast and mitochondrion, were difficult. The tonoplast fractions were distinctly different from other fractions (Fig. 4c) and had a greater relative density compared to

bioRxiv preprint doi: https://doi.org/10.1101/2023.04.21.537482; this version posted April 23, 2023. The copyright holder for this preprint (which was not certified by peer review) is the author/funder, who has granted bioRxiv a license to display the preprint in perpetuity. It is made available under aCC-BY-NC-ND 4.0 International license.

that found in Arabidopsis[56] and other glycophyte species, where the tonoplast is the least dense membrane. This apparently higher density of the tonoplast in *S. bigelovii* is supported not only by the western blot analysis (Fig. 4a), but also by the abundance profiles of tonoplast marker proteins such as vacuolar ATPase subunits and the vacuolar pyrophosphatase (Fig. 4c, Supplementary Figs. 9-11, and Supplementary Data File 6). This higher density may be due to higher levels of membrane proteins in the tonoplast, perhaps related to the very high concentration of ions accumulating in the vacuoles of *Salicornia* shoots.

bioRxiv preprint doi: https://doi.org/10.1101/2023.04.21.537482; this version posted April 23, 2023. The copyright holder for this preprint (which was not certified by peer review) is the author/funder, who has granted bioRxiv a license to display the preprint in perpetuity. It is made available under aCC-BY-NC-ND 4.0 International license.

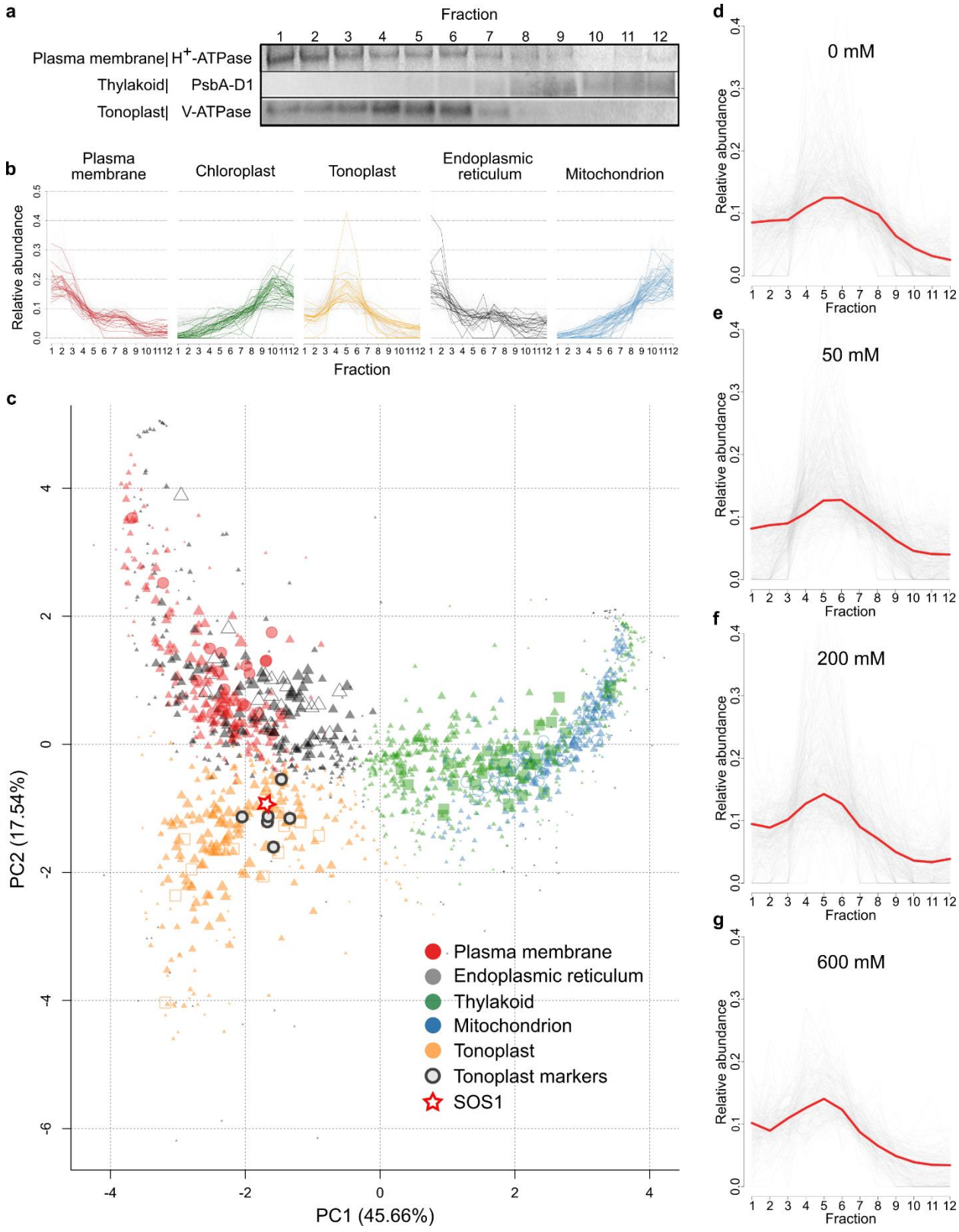

bioRxiv preprint doi: https://doi.org/10.1101/2023.04.21.537482; this version posted April 23, 2023. The copyright holder for this preprint (which was not certified by peer review) is the author/funder, who has granted bioRxiv a license to display the preprint in perpetuity. It is made available under aCC-BY-NC-ND 4.0 International license.

Figure 4. Spatial protein profiles and validation of marker abundance profiles generated with pRoloc from membrane preparations from shoots of *S. bigelovii* plants treated with 200 mM NaCl. **a,** Western blot analyses of organelle marker proteins for the plasma membrane (H^+-ATPase), thylakoid (PsbA-D1), and tonoplast (V-ATPase) on 5 µg of proteins from each of the 12 density fractions. **b,** Relative protein abundance profiles identified with pRoloc of organelle marker proteins on the 12 density fractions. **c,** Principal component analysis of protein predicted subcellular localization by pRoloc. The size of the symbol represents confidence values of localization. Plasma membrane: red, markers as circles; endoplasmic reticulum: grey, markers as open triangles; chloroplast: green, markers as squares; mitochondrion: blue, markers as open circles; tonoplast: orange, markers as open squares; tonoplast marker proteins, encircled in black: Vacuolar ATPase subunits a, b, c and d, Vacuolar pyrophosphatase, and Tonoplast intrinsic protein 1-3; and red star, SOS1. **d-g,** Relative protein abundance profiles of SOS1 (red) and proteins allocated to the tonoplast (grey) at different treatments. **d,** 0 mM NaCl. **e,** 50 mM NaCl. **f,** 200 mM NaCl. **g,** 600 mM NaCl.

Possible neo-localization of SOS1 to the tonoplast in *S. bigelovii*

Exploration of the organellar membrane proteome revealed the localization of SOS1, also known as NHX7, to the tonoplast (Fig. 4c-g). SOS1 was first identified in Arabidopsis[46,71] and has been described as a Na^+/H^+ antiporter localized to the plasma membrane, extruding Na^+ from the cytosol into the apoplast[46,72-74]. SbiSOS1 is predicted to be 1159 amino acids in length, the same as the predicted SOS1 sequence

bioRxiv preprint doi: https://doi.org/10.1101/2023.04.21.537482; this version posted April 23, 2023. The copyright holder for this preprint (which was not certified by peer review) is the author/funder, who has granted bioRxiv a license to display the preprint in perpetuity. It is made available under aCC-BY-NC-ND 4.0 International license.

in *S. europaea* and the reported SOS1 sequence for *S. brachiata*[75]. SbiSOS1 clustered with SOS1-like proteins (Fig. 2c) and shows a 63% sequence identity to Arabidopsis SOS1 and only a 27% identity to other NHX proteins. Similar sequence identities can be observed between the SOS1 protein of Arabidopsis and those of Quinoa, Rice, and Tomato (61-63%). Protein abundance profiles show that SbiSOS1 localizes to the tonoplast. This was consistent across all treatments, and in all instances, it had a high allocation score to the tonoplast (Fig. 4d-g, Supplementary Figs. 9-11, Supplementary Data File 6). Furthermore, it was closely distributed with tonoplast marker proteins such as: vacuolar ATPase subunits a, b, c, d; tonoplast intrinsic protein TIP1-3; and the vacuolar pyrophosphatase (Fig. 4c, Supplementary Figs. 9-11). SbiSOS1 was more abundant in fractions 4-6 (Fig. 4d-g), following the abundance pattern of tonoplast marker proteins and different to plasma membrane markers (Fig. 4a,b). SbiSOS1 was amongst the most abundant membrane proteins in shoots of *S. bigelovii*, together with the plasma membrane H^+-ATPase, the vacuolar V-ATPases, PIPs, and TIPs (Supplementary Data File 6), and its abundance did not change with treatment. These results suggest the localization of SOS1 to the tonoplast in *S. bigelovii* and a high and constitutive abundance of SbiSOS1 in these cells. SbiSOS1 may have a role for rapid Na^+ sequestration into the vacuole, enabling the cells to accumulate high Na^+ concentrations.

NaCl increases the abundance of membrane proteins related to ATP synthesis

bioRxiv preprint doi: https://doi.org/10.1101/2023.04.21.537482; this version posted April 23, 2023. The copyright holder for this preprint (which was not certified by peer review) is the author/funder, who has granted bioRxiv a license to display the preprint in perpetuity. It is made available under aCC-BY-NC-ND 4.0 International license.

We then looked at the protein responses upon salt treatment. Of the 2,118 unique protein clusters, 687 were found to be differentially abundant in at least one of the treatments (Supplementary Fig. 12 and Supplementary Data File 6). Hierarchical clustering of the differentially abundant proteins showed a clear two-group clustering between replicates from each treatment and between plants treated with 0 and 50 mM NaCl and those treated with 200 and 600 mM NaCl (Supplementary Fig. 12). GO enrichment analysis of proteins significantly more abundant in plants treated with 200 and 600 mM NaCl revealed enrichment in the terms ‘cellular respiration’, ‘ATP synthesis’, ‘generation of precursor metabolites and energy’, and ‘cellular nitrogen compound biosynthetic process’, among others (Supplementary Data File 5). Indicating that plants treated with higher concentrations of NaCl have higher rates of respiration and growth. Plants grown in 0 mM and 50 mM were enriched in the terms ‘programmed cell death’, ‘organelle fusion’, and ‘calcium ion homeostasis’ (Supplementary Data File 5), indicating that plants grown under suboptimal NaCl concentrations were stressed. MapMan pathway enrichment analysis produced similar results, suggesting increased signaling and vesicle trafficking in plants grown in 0 mM and 50 mM NaCl and an increase in ribosome biogenesis and ATP synthesis in plants treated with 200 and 600 mM NaCl (Supplementary Tables 5 and 6).

Identification of salt tolerance related genes in yeast

To identify genes of *S. bigelovii* involved in salt tolerance, genes were selected for salt tolerance assays in the salt sensitive yeast strain AXT3 (Δena1-4::HIS3 Δnha1::LEU2 Δnhx1::TRP1)[76] based on the following criteria: 1) Genes which were differentially expressed in response to NaCl; 2) Genes previously associated with salinity tolerance;

bioRxiv preprint doi: https://doi.org/10.1101/2023.04.21.537482; this version posted April 23, 2023. The copyright holder for this preprint (which was not certified by peer review) is the author/funder, who has granted bioRxiv a license to display the preprint in perpetuity. It is made available under aCC-BY-NC-ND 4.0 International license.

3) Genes with a domain or description associated with Na, K, Cl, or Ca; and 4) Preference was given to transmembrane proteins predicted to have at least six transmembrane helices, as this would advocate for transporters and channels. Based on these criteria, 45 genes were cloned and 11 showed a phenotype in response to NaCl (Fig. 5, Supplementary Fig. 13, Supplementary Table 7, Supplementary Data File 7). *SbiSOS1* was toxic to *E. coli* and we were not able to retrieve a functional transformant for its further analysis in yeast.

Increased salinity tolerance was observed for four genes: *SbiKAT2*, *SbiNHX4*, *SbiOPT4*, and *SbiSALTY* (Fig. 5a and Supplementary Fig. 13). *SbiKAT2* is similar to Arabidopsis potassium channel *KAT2*. It was downregulated upon NaCl treatment, it greatly increased yeast salt tolerance, and its activity as a K^+ channel was confirmed when grown in high concentrations of K^+, leading to K^+ toxicity and cell death (Supplementary Fig. 14). *NHX* genes showed different phenotypes in yeast but were not differentially expressed in *S. bigelovii* upon NaCl treatment. *SbiNHX4* greatly increased yeast salt tolerance and is similar to Arabidopsis *NHX4*, belonging to the Class I exchangers (NHX1-NHX4) that are localized to the tonoplast[42-44] and are considered to be primarily responsible for the compartmentalization of K^+ in the vacuole[77-80]. SbiOPT4 is similar to the oligopeptide transporter OPT4 in Arabidopsis, which has been described as a proton/oligopeptide transporter[81]. *SbiOPT4* expression increased upon NaCl treatment and conferred a moderate increase in salinity tolerance in yeast, particularly when grown in AP medium (Supplementary Fig. 13). The most pronounced phenotype was observed with an RGG protein, which we called SALTY. Its gene expression and protein abundance increased upon NaCl treatment, and it localized to

bioRxiv preprint doi: https://doi.org/10.1101/2023.04.21.537482; this version posted April 23, 2023. The copyright holder for this preprint (which was not certified by peer review) is the author/funder, who has granted bioRxiv a license to display the preprint in perpetuity. It is made available under aCC-BY-NC-ND 4.0 International license.

the cytosol in yeast (Supplementary Figs. 11 and 15). RGG proteins are not well studied in plants. Sequence analysis of SbiSALTY suggested it to be an intrinsically disordered protein (IDP), a protein that does not have a defined three-dimensional structure. The overexpression of Arabidopsis homologs AtRGGA (AT4G16830) and the RGG protein (AT4G17520) also increased salt tolerance in yeast, albeit to a lesser extent (Fig. 5a,c).

Reduced salt tolerance in yeast was observed for seven genes: *SbiHKT1*, *SbiNHX1*, *SbiNHX2*, *SbiENT1*, *SbiSLC5-6*, *SbiPQ*, and *SbiIDP1* (Fig. 5b and Supplementary Fig. 13). Expression of *SbiHKT1* decreased with NaCl treatment (Fig. 3e) and its induction in yeast led to cell death. HKT1;1 has been reported to be involved in root Na^+ accumulation and Na^+ retrieval from the xylem, preventing Na^+ accumulation in leaves of Arabidopsis[52,53]. Two *NHX* genes (*SbiNHX1* and *SbiNHX2*) decreased salt tolerance in yeast, contrarily to what was observed for *SbiNHX4*. This may be due to differences in their subcellular localization in yeast, with SbiNHX1 and SbiNHX2 primarily localizing to lysosomes and SbiNHX4 to the vacuole and ER (Supplementary Fig. 16). *SbiENT1* is similar to Arabidopsis equilibrative nucleoside transporter 1 (ENT1). It was predicted to be localized to the tonoplast and was upregulated upon NaCl treatment. Equilibrative nucleoside transporters mediate the transport of purine and pyrimidine nucleosides[82]. In Arabidopsis, ENT1 is localized to the tonoplast and its overexpression leads to stunted growth[83]. *SbiSLC5-6* expression did not change upon NaCl treatment and was predicted to localize to the tonoplast. It resembles a sodium-coupled amino acid transporter and has an SLC5-6-like_sbd superfamily domain. SLC5 proteins cotransport Na^+ and a substrate, usually glucose[84], whereas SLC6 proteins utilize Na^+ and Cl^- to cotransport substrates[85]. *SbiPQ* expression did not

bioRxiv preprint doi: https://doi.org/10.1101/2023.04.21.537482; this version posted April 23, 2023. The copyright holder for this preprint (which was not certified by peer review) is the author/funder, who has granted bioRxiv a license to display the preprint in perpetuity. It is made available under aCC-BY-NC-ND 4.0 International license.

change upon NaCl treatment and it is similar to the PQ-loop repeat family of proteins. PQ-loop proteins are not well studied in plants, but have recently been shown to function as H^+/monovalent cation transporters in plants[86] and as H^+/amino acid transporters in yeast[87] and human[88,89]. *SbiIDP1* was upregulated upon NaCl treatment and greatly induced yeast cell death, particularly upon NaCl treatment. It had no significant similarity to any Arabidopsis protein, and similarly to SbiSALTY, it is predicted to be an intrinsically disordered protein, to form coiled coils, and was localized to the cytosol in yeast (Supplementary Fig. 17).

bioRxiv preprint doi: https://doi.org/10.1101/2023.04.21.537482; this version posted April 23, 2023. The copyright holder for this preprint (which was not certified by peer review) is the author/funder, who has granted bioRxiv a license to display the preprint in perpetuity. It is made available under aCC-BY-NC-ND 4.0 International license.

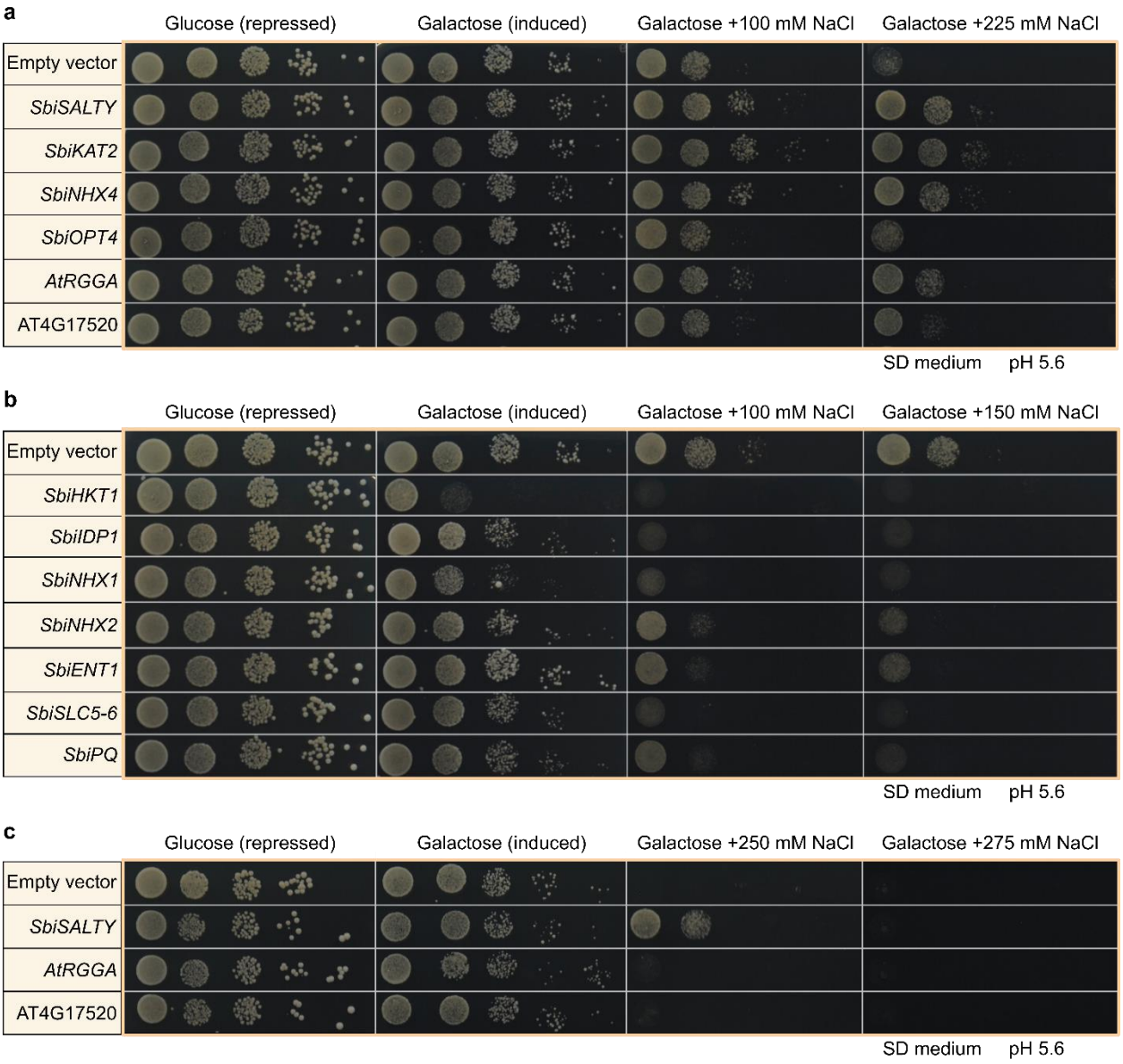

Figure 5. Yeast spot assays in AXT3 strain at different NaCl treatments. **a,** genes increasing salt tolerance. **b,** genes decreasing salt tolerance. **c,** RGG proteins at high NaCl. Assays were done in SD medium pH 5.6 and supplemented with 2% galactose for gene induction.

bioRxiv preprint doi: https://doi.org/10.1101/2023.04.21.537482; this version posted April 23, 2023. The copyright holder for this preprint (which was not certified by peer review) is the author/funder, who has granted bioRxiv a license to display the preprint in perpetuity. It is made available under aCC-BY-NC-ND 4.0 International license.

The RGG protein SALTY is an intrinsically disordered protein and is localized to the ER

We further characterized SbiSALTY, as it greatly increased salt tolerance in yeast. Sequence analyses suggests it to be an intrinsically disordered protein (Fig. 6a, Supplementary Fig. 18) and be able to form coiled-coils (Fig. 6b), which could allow for oligomerization. To confirm its structure, SbiSALTY was expressed and purified in *E. coli* for circular dichroism (CD) and NMR analysis. The CD spectrum showed that SbiSALTY is predominantly disordered, having a minimum around 200 nm and very low ellipticity above 210 nm[90,91], missing both well-pronounced classical secondary structures and distinct tertiary structural motifs (Fig. 2c). Temperature-based CD analyses at three different wavelengths, 201, 208, and 222 nm, showed no significant alterations at temperatures ranging from 20 to 92 °C (Fig. 2d), supporting the notion that SbiSALTY is an IDP. To explore the detailed structure of SbiSALTY, we expressed and purified the uniformly ^{15}N-labelled protein for NMR analysis. The acquired high-resolution 2D ^{1}H-^{15}N TROSY-HSQC spectrum indicates that SbiSALTY is an IDP as the signal dispersion is minimal, particularly in the ^{1}H dimension (Fig. 2e). This minimal dispersion is typical of IDPs[92,93]. The overall number of identified ^{1}H/^{15}N backbone amide correlations found in the spectrum fits the expected amount based on the SbiSALTY primary structure, confirming the one dominant conformation of the disordered state of the intact protein in solution. We did not observe any ^{1}H/^{15}N chemical shift changes with concentrations ranging from 50 µM to 1 mM. These data suggest that SbiSALTY is water-soluble and intrinsically disordered.

bioRxiv preprint doi: https://doi.org/10.1101/2023.04.21.537482; this version posted April 23, 2023. The copyright holder for this preprint (which was not certified by peer review) is the author/funder, who has granted bioRxiv a license to display the preprint in perpetuity. It is made available under aCC-BY-NC-ND 4.0 International license.

Since SbiSALTY is a water-soluble protein, its abundance in our membrane proteomes was highly diminished and its allocation to a subcellular compartment should be taken with caution. Nevertheless, SbiSALTY was detected and was most abundant at higher NaCl treatments and in proximity to ribosomal proteins (Supplementary Fig. 11). Expression of *SbiSALTY* in rice protoplasts suggests its localization to the ER, as it co-localized with an ER marker (Fig. 6i-l). The homolog of this gene in Arabidopsis (*RGGA*, AT4G16830) was observed to localize to the cytosol and interact with non poly-A RNA[94], suggesting it might interact with ribosomes. Ribosomes bound to the ER (rough ER) cause an increase in the membrane's density when compared to the ribosomes-devoid smooth ER, leading to an increased specific gravity between 1.15 – 1.18[95,96], where SbiSALTY was most abundant. Most ribosomal proteins were also identified across these fractions. Sequence analysis of SbiSALTY with Phyre2[97] predicted it to be a highly disordered protein, but showed a short conserved not disordered region to be most similar to the 40S ribosomal protein S7 (Supplementary Fig. 18). This small, conserved region falls within the region predicted to form coiled-coils and could help SbiSALTY interact with ribosomes in the ER of plants.

bioRxiv preprint doi: https://doi.org/10.1101/2023.04.21.537482; this version posted April 23, 2023. The copyright holder for this preprint (which was not certified by peer review) is the author/funder, who has granted bioRxiv a license to display the preprint in perpetuity. It is made available under aCC-BY-NC-ND 4.0 International license.

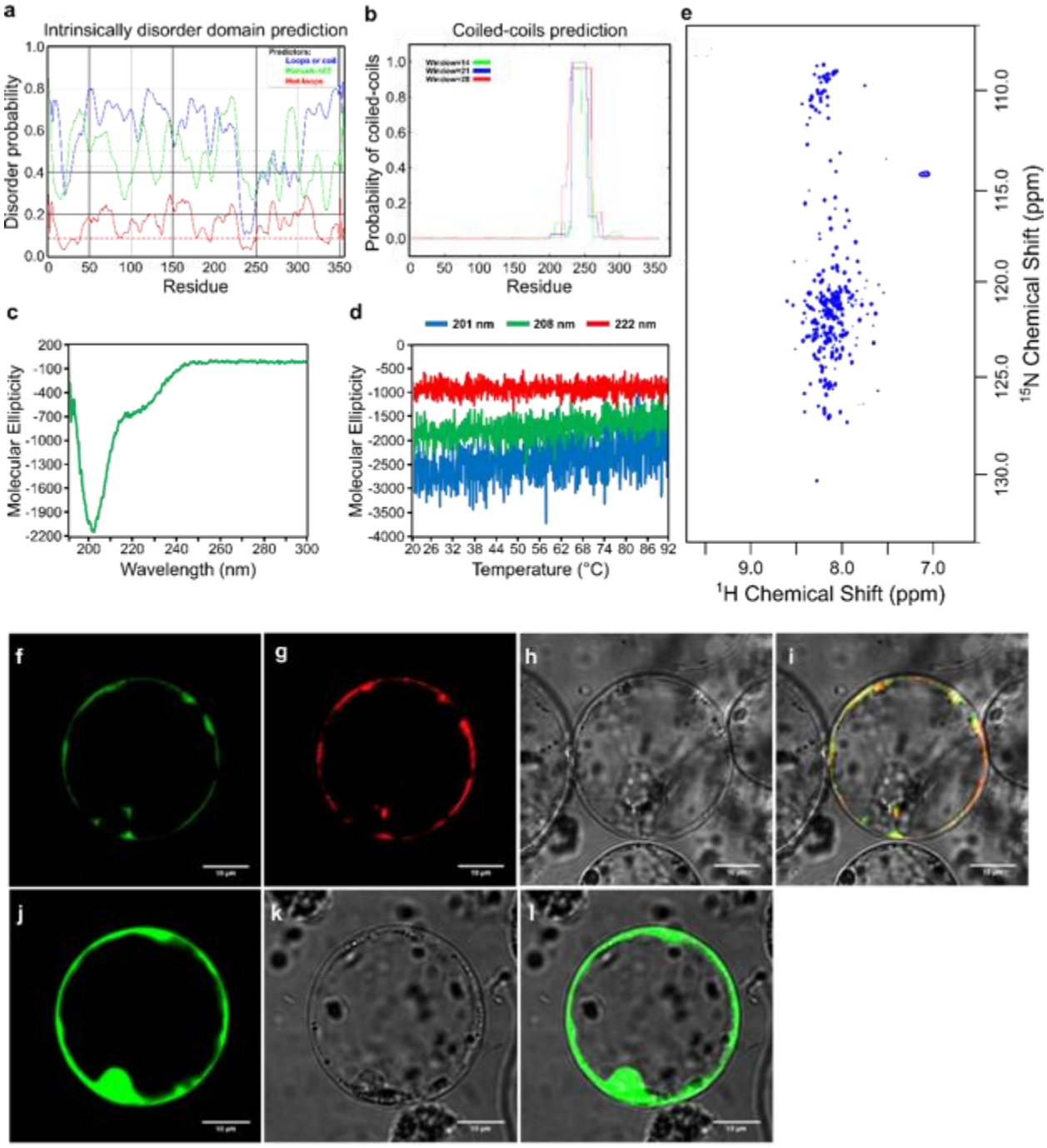

Figure 6. Structure prediction for SbiSALTY and its subcellular localization in rice protoplasts. **a,** Intrinsically disordered domain prediction. Dotted lines represent random expectation values for each model. **b,** Coiled-coils prediction. **c,** CD measurements of SbiSALTY at 30℃. Wavelength range from 190 nm to 260 nm showing secondary

bioRxiv preprint doi: https://doi.org/10.1101/2023.04.21.537482; this version posted April 23, 2023. The copyright holder for this preprint (which was not certified by peer review) is the author/funder, who has granted bioRxiv a license to display the preprint in perpetuity. It is made available under aCC-BY-NC-ND 4.0 International license.

structure and wavelength range from 250 nm to 300 nm showing tryptophan and tertiary structure. **d,** Temperature melting curve analysis of 201 nm, 208 nm and 222 nm of SbiSALTY in CD ranging from 20 – 92 °C. **e,** ^{1}H-^{15}N HSQC spectrum of SALTY-WT in 800 MHz NMR analysis**. f-l,** protein expression in rice protoplasts. **f,** SbiSALTY-EGFP. **g,** ER-marker-RFP. **h,** Bright field. **i,** Merged image. **j,** empty vector expressing EGFP. **k,** Bright field. **l,** Merged image.

Discussion

Here we studied the responses of the highly salt tolerant *S. bigelovii* to NaCl and generated the first genomic resources for the genus *Salicornia*. These plants are able to accumulate very high concentrations of NaCl in their shoot whilst avoiding visible symptoms of ion toxicity. Nevertheless, *S. bigelovii* plants displayed enhanced growth upon the addition of NaCl and accumulated very high concentrations of Na^+ and Cl^- in its shoots and roots (Fig. 1).

The positive effect of NaCl on growth was also observed at a transcriptional and protein level, where genes and proteins related to growth, photosynthesis, cell wall modification, water transport, and ATP synthesis were found to be upregulated upon NaCl treatment. The high concentration of both Na^+ and Cl^- in shoots and its positive correlation with water content suggest a possible role for both ions as osmolytes. Na^+ was found to be more effective than Cl^- or K^+ for supporting *S. europaea* growth[98]. Nevertheless, a set of adaptations and possibly a tight regulation of specialized ion transporters would be required to avoid ion toxicity, moving ions out of the cytosol, and in particular into the large volume of the vacuole.

bioRxiv preprint doi: https://doi.org/10.1101/2023.04.21.537482; this version posted April 23, 2023. The copyright holder for this preprint (which was not certified by peer review) is the author/funder, who has granted bioRxiv a license to display the preprint in perpetuity. It is made available under aCC-BY-NC-ND 4.0 International license.

Gene ontology enrichment analysis of unique orthogroups in *Salicornia* revealed enrichment in terms related to responses to high light intensity, toxin metabolism and ion channel activity, in the form of calcium channels. These calcium channels could help in calcium signaling upon NaCl stress, allowing for a fast response. However, neither an enrichment specific to Na^+ transport nor an expansion in known Na^+ transporters were observed. Suggesting that *Salicornia* might use the same set of genes found in other plants, albeit adapted for highly saline environments, or possess genes involved in salinity tolerance that have not yet been discovered.

Analysis of the organellar membrane proteomes revealed a possible neo-localization of SOS1 to the tonoplast (Fig. 4). SbiSOS1 was highly abundant in all treatments and was always allocated with high confidence to the tonoplast in our organellar membrane proteomes. SOS1 has been described as a plasma membrane Na^+/H^+ antiporter localized to the plasma membrane in Arabidopsis, where it transports Na^+ outside of the cell[46,71-74]. Its localization to the tonoplast in *S. bigelovii* could allow for high concentrations of Na^+ to be compartmentalized into the vacuole, preventing Na^+ from causing toxicity in the cytoplasm, and allowing its use as an osmolyte for water retention. Such compartmentalization of Na^+ in the vacuole would be advantageous in highly saline environments, as the otherwise continuous Na^+ extrusion from the cytoplasm to the extracellular space would be highly energetically demanding. V-ATPases, vacuolar pyrophosphatases, and TIPs were amongst the most abundant proteins in our membrane proteomes. The V-ATPase and vacuolar pyrophosphatases would generate H^+ ions to be used by the Na^+/H^+ antiporter activity of SOS1[99], while the

bioRxiv preprint doi: https://doi.org/10.1101/2023.04.21.537482; this version posted April 23, 2023. The copyright holder for this preprint (which was not certified by peer review) is the author/funder, who has granted bioRxiv a license to display the preprint in perpetuity. It is made available under aCC-BY-NC-ND 4.0 International license.

TIPs would allow water flow into the vacuole, helping the increase in volume of *Salicornia* vacuoles that occurs in response to elevated salinity.

We identified 11 proteins that showed a phenotype in yeast – four increased salt tolerance and seven decreased it. Two NHX proteins decreased salt tolerance (SbiNHX1 and SbiNHX2), while one greatly increased it (SbiNHX4), which could be related to their different subcellular localization in yeast. Alternatively, their predicted C-terminus localization with respect to the membrane was opposite in SbiNHX4 when compared to SbiNHX1 and SbiNHX2 and could play a role in their regulation, as the binding of proteins to the C-terminus can influence their activities[100,101]. We also identified an *SbiHKT1* whose expression was reduced *in planta* upon NaCl treatment, and which led to cell death in yeast. *In planta*, HKT1 seems likely to reduce root-to-shoot translocation of Na^+ by removing Na^+ from the transpiration stream into xylem parenchyma cells[102].

Two predicted intrinsically disordered proteins, SbiIDP1 and SbiSALTY, showed contrasting phenotypes in yeast. SbiSALTY is an Arginine-Glycine-Glycine (RGG) motif protein and greatly increased salt tolerance in yeast. RGG proteins are not well studied in plants, but in humans are known to be RNA binding proteins[103-105]. In Arabidopsis, the overexpression of *AtRGGA,* encoding an RGG protein, increased salt and drought tolerance compared to wild type plants. The protein localized to the cytosol, and bound non poly-A RNA[94]. Expression of Arabidopsis homologs *RGGA* and *AT4G17520* in yeast also increased salt tolerance, albeit to a lesser extent than SbiSALTY (Fig. 5). NMR and CD analyses confirmed SbiSALTY to be an intrinsically disordered protein. Some of the most commonly known IDPs are the Late Embryogenesis Abundant (LEA)

bioRxiv preprint doi: https://doi.org/10.1101/2023.04.21.537482; this version posted April 23, 2023. The copyright holder for this preprint (which was not certified by peer review) is the author/funder, who has granted bioRxiv a license to display the preprint in perpetuity. It is made available under aCC-BY-NC-ND 4.0 International license.

proteins, which are involved in dehydration tolerance[106-108]. IDPs are considered to be primary constituents of membrane-less compartments within the cell[109-111]. Membrane-less compartments display liquid-like properties[112] and form structures such as stress granules and p-bodies, which have been observed to contain ribosomal subunits and translation initiation factors[113-115]. In our membrane proteomes, SbiSALTY was found to be most abundant at densities where ribosomal proteins are found and the expected density of the rough ER. However, a precise localization of SbiSALTY in our proteomes is difficult, as soluble protein abundances were reduced during membrane enrichment and no Mg^{2+} was added to our density fractions to preserve the ribosomes binding to the ER[95,96]. Nevertheless, *in planta*, SbiSALTY was found to be localized to the ER. The intrinsically disordered nature of SbiSALTY, together with its predicted ability to form coiled-coils at a region highly similar to the 40S ribosomal proteins S7, could provide it with the required flexibility to form part of membrane-less compartments, where it could bind to RNA-containing structures such as ribosomes, possibly stabilizing or protecting them during salt stress.

The analyses presented in this study provide new insights into the responses of *S. bigelovii* to salinity and the possible adaptations and mechanisms that allow it to thrive in highly saline environments. The resources generated open the possibility for further research in *Salicornia*, which will increase our knowledge of salinity tolerance and will help in the development of salt tolerant crops.

Methods

bioRxiv preprint doi: https://doi.org/10.1101/2023.04.21.537482; this version posted April 23, 2023. The copyright holder for this preprint (which was not certified by peer review) is the author/funder, who has granted bioRxiv a license to display the preprint in perpetuity. It is made available under aCC-BY-NC-ND 4.0 International license.

Plant material and growth conditions

Salicornia bigelovii seeds were kindly provided by Dr. E. Glenn of the Environmental Research Laboratory, University of Arizona, Tucson, USA. *Salicornia europaea* seeds were collected in the Dead Sea area and were kindly provided by Dr. Moshe Sagi of the Blaustein Institute for Desert Research (BIDR), Israel. For phenotypic, transcriptomic, and proteomic experiments in *S. bigelovii*, seeds derived from inbred populations were sown in Metro-Mix® 360 soil (SunGro Horticulture, USA) contained in plastic trays and watered daily to 70% soil water holding capacity. *S. bigelovii* plants of one inbred line were grown during the months of May – July 2015 in a glasshouse in KAUST under natural irradiance and kept at a constant temperature of 28/24°C day/night with 65% relative humidity. Five weeks after sowing, *S. bigelovii* plants were treated with saline water to reach a final concentration of 0, 5, 50, 200, or 600 mM NaCl in the soil.

Plant phenotype and ion content

Shoot diameter imaging and measurements were obtained by finely slicing *S. bigelovii* shoots with a surgical blade and examining them under a light microscope (AZ100 Multizoom, Nikon, Japan). Shoot area cross sections were measured with NIS-Elements BR software (Nikon). For ion content, shoots and roots of *S. bigelovii* were harvested 1 and 6 weeks after salt treatment. Samples were rinsed with MilliQ water and had the surface water removed with paper towels prior to fresh mass measurements. Samples were then dried in an oven at 70 °C for 3 days and had their dry mass measured. 10 mg of dried tissue were mixed with 1.5 mL of 500 mM nitric

bioRxiv preprint doi: https://doi.org/10.1101/2023.04.21.537482; this version posted April 23, 2023. The copyright holder for this preprint (which was not certified by peer review) is the author/funder, who has granted bioRxiv a license to display the preprint in perpetuity. It is made available under aCC-BY-NC-ND 4.0 International license.

acid, heated at 80 °C for 3 h, and used for Na and K content analyses by flame photometry (Flame photometer model 420, Sherwood Scientific Ltd, United Kingdom) and Cl^- content (Chloride analyser model 926, Sherwood Scientific Ltd, United Kingdom). Flame photometry measures the total element in a sample, not distinguishing between ionic and non-ionic forms; nevertheless, these measurements will be referred to as "Na^+" and "K^+" and not as "Na" and "K" as most of these elements are found as ions in the cell. In contrast, the choride analyzer uses titration with silver nitrate to measure chloride in its ionic form, "Cl^-". Water content was calculated as (fresh mass – dry mass) / dry mass. Shoot sap osmolality was obtained by crushing *S. bigelovii* shoots and centrifuging at 10,000 x *g* for 2 minutes. 10 µL of the supernatant was measured with a VAPRO® (ELITechGroup). For mean comparison across treatments, statistical analyses of three samples per treatment were done with the R package stats v.3.6.3[116].

DNA extraction, library preparation, and sequencing

High molecular weight (HMW) DNA was isolated from the young secondary stems of a single plant after dark-treatment for 48 hours. DNA was isolated using a modified CTAB method. Briefly, 5 grams of tissue were combined with 10 mL of CTAB Buffer (2% (w/v) CTAB, 1.4 M NaCl, 100 mM Tris-HCl (pH 8), 20 mM EDTA (pH 8), 2% (w/v) PVP (MW 10,000), 1% (v/v) Triton X-100, 0.1% (v/v) βME, 1.9 mg/mL RNase-A, and 10 mg/mL proteinase K). Extracts were incubated and mixed for 45 min at 65°C before isolation of the aqueous phase with chloroform:isoamyl alcohol (24:1), done thrice. The DNA was precipitated in 0.6 volumes of pure isopropyl alcohol. The HMW DNA was pelleted and washed with 70% (v/v) ethanol and resuspended in TE buffer (pH 8.0). HMW DNA was

bioRxiv preprint doi: https://doi.org/10.1101/2023.04.21.537482; this version posted April 23, 2023. The copyright holder for this preprint (which was not certified by peer review) is the author/funder, who has granted bioRxiv a license to display the preprint in perpetuity. It is made available under aCC-BY-NC-ND 4.0 International license.

further purified using AMPure PB beads (Beckman Coulter, USA) and resuspended in TE buffer (pH 8.0). High molecular weight DNA was used for HiFi sequencing of 4 PacBio HiFi SMRT cells, accounting for 57,386,832,994 bp or ~28x coverage for *S. bigelovii* and 2 PacBio HiFi SMRT cells, accounting for 17,950,298,972 bp or ~34x coverage for *S. europaea* and were sequenced in a PacBio Sequel II system at The Arizona Genomics Institute of The University of Arizona (USA). For genome size estimation using *k*-mer analysis, Illumina per species were sequenced in a NovaSeq 6000 system at The Arizona Genomics Institute of The University of Arizona (USA), resulting in 112,237,052,136 bp or ~55x coverage for *S. bigelovii* and 29,229,294,386 bp or ~56x coverage for *S. europaea*.

RNA extraction and library preparation

To generate reference transcriptomes for gene annotation, RNA samples from shoots and roots from *S. bigelovii* and *S. europaea* were extracted with an RNeasy Plant Mini Kit (Qiagen). RNA quality was determined with a Bioanalyzer 2100 using an RNA 600 Nano kit (Agilent, USA). High quality of RNA was used to prepare RNA-Seq libraries with NEBNext® Ultra™ Directional RNA Library Prep Kit for Illumina® (New England BioLabs, USA) according to the manufacturer's instructions. RNA-Seq libraries were sequenced in a NovaSeq 6000 system (Illumina, USA) under paired-end mode and 151 bp read length at the Bioscience Core Labs (KAUST), resulting in 552 million (~83 Gb) and 488 million (~73 Gb) reads for *S. bigelovii* and *S. europaea*, respectively.

For gene differential expression analysis of shoots for *S. bigelovii* plants treated with 0, 50, 200, or 600 mM NaCl for 1 and 6 weeks, RNA was extracted with TRIzol™

bioRxiv preprint doi: https://doi.org/10.1101/2023.04.21.537482; this version posted April 23, 2023. The copyright holder for this preprint (which was not certified by peer review) is the author/funder, who has granted bioRxiv a license to display the preprint in perpetuity. It is made available under aCC-BY-NC-ND 4.0 International license.

and an RNA MiniPrep kit (Zymo Research, USA), following the manufacturer's protocol. RNA quality was determined with a Bioanalyzer 2100 using an RNA 600 Nano kit (Agilent, USA) using only RNA with RIN values greater to 8. Libraries for RNA-Seq were prepared with NEBNext® Ultra™ Directional RNA Library Prep Kit for Illumina® (New England BioLabs, USA) for three replicates per treatment resulting in 24 libraries with a mean insert size of 300 bp. DNA quality was determined with a high sensitivity DNA kit (Agilent, USA) using a Bioanalyzer 2100. Libraries were barcoded and sequenced in two lanes of Illumina HiSeq 2000 generating ~540 million paired end reads of 2x101 bp or ~22.5 million reads per library (Supplementary Data File 4) at the Bioscience Core Labs (KAUST, Saudi Arabia).

Chromosome counting and genome size estimation

To count the number of chromosomes of *S. bigelovii* and *S. europaea*, chromosome spreads were prepared from actively growing roots as previously described[117] with minor modifications. Roots were collected into 50 mM phosphate buffer (pH 7.0) containing 0.2% (v/v) β-mercaptoethanol. The roots were transferred to 0.05% (w/v) 8-hydroxyquinoline and incubated for three hours at room temperature, fixed in 3:1 ethanol:acetic acid fixative and stored in 70% (v/v) ethanol at -20 °C for further use. At least twenty roots were washed three times with distilled water within 10 min and once in 1xKCl buffer (pH 4.0) for 5 min. Meristematic zones of the roots were excised and digested in 200 µl of the enzyme solution containing 4% (w/v) cellulase and 1% (v/v) pectolyase for 48 min at 37 °C, then 200 µL of TE buffer (pH 7.6) was added to stop the reaction. Root partitions were washed three times in 96% (v/v) ethanol and 25 µL of 9:1

bioRxiv preprint doi: https://doi.org/10.1101/2023.04.21.537482; this version posted April 23, 2023. The copyright holder for this preprint (which was not certified by peer review) is the author/funder, who has granted bioRxiv a license to display the preprint in perpetuity. It is made available under aCC-BY-NC-ND 4.0 International license.

ice-cold acetic acid: methanol mixture was added. The root tips were broken with a rounded dissecting needle and the tube was kept on ice for 5 min before dropping. The suspension (5 µL) was dropped onto microscopic slide placed in a humid polystyrene box. The preparations were air-dried and counterstained with DAPI mounted in VECTASHIELD Antifade Mounting Medium (Vector Laboratories, Burlingame, CA, USA). The slides were examined with an Axio Imager Z.2 Zeiss microscope (Zeiss, Oberkochen, Germany). Pictures were captured by the ISIS software 5.4.7 (Metasystems) and chromosomes were counted manually. A minimum of five mitotic metaphase plates per slide were captured. Genome sizes were estimated through flow cytometry and *k*-mer frequencies. Nuclear DNA content was estimated by flow cytometry from three different individual inbred plants per species, as previously described[118], using *Zea mays* L. 'CE-777 (2C = 5.43 pg DNA) and *Solanum lycopersicum* L. 'Stupické polní rané' (2C = 1.96 pg DNA) as internal reference standards for *S. bigelovii* and *S. europaea*, respectively. Samples were analyzed using a CyFlow Space flow cytometer (Sysmex Partec GmbH, Görlitz, Germany) equipped with a 532 nm laser. The gain of the instrument was adjusted so that the peak representing G1 nuclei of the standard was positioned approximately on channel 100 (*Zea mays*) or 170 (*Solanum lycopersicum*) on a histogram of relative fluorescence intensity when using a 512-channel scale. Three individual plants were sampled and analyzed three times. At least 5000 nuclei per sample were analyzed and 2C nuclear DNA contents were calculated from means of G1 peak positions by applying the formula: 2C nuclear DNA content = (sample G1 peak mean) × (standard 2C DNA content) / (standard G1 peak mean). The mean nuclear DNA content in pg was

bioRxiv preprint doi: https://doi.org/10.1101/2023.04.21.537482; this version posted April 23, 2023. The copyright holder for this preprint (which was not certified by peer review) is the author/funder, who has granted bioRxiv a license to display the preprint in perpetuity. It is made available under aCC-BY-NC-ND 4.0 International license.

converted to genome size in bp using the conversion factor 1pg DNA = 0.978 Gbp[118]. Genome size estimation through *k*-mer frequencies was done with FindGSE[27] by counting *k*-mer frequencies of Illumina or HiFi reads with Jellyfish[119]. For genome size estimation with Illumina reads, reads were first trimmed with Trimmomatic[120] and quality checked with FastQC[121] prior to *k*-mer analysis.

Genome assembly and annotation

The genomes of *S. bigelovii* and *S. europaea* were assembled using the PacBio HiFi reads with HiFiasm[122]. HiFiasm was run with the --n-hap 4 and -s 0.35 commands for *S. bigelovii* and with the -s 0.35 command for *S. europaea*. The genome assembly completeness was measured with Merqury[28], resulting in 97.13% and 99.29% read *k*-mer presence in the genome assemblies for *S. bigelovii* and *S. europaea*, respectively. The genomes of the *Salicornia* species were masked for repetitive elements by generating a *de novo* repeat library with RepeatModeler for each species and used to mask the genome with RepeatMasker[123-125]. Hints for genome annotation were generated by mapping RNA-Seq data from each species into their corresponding genome with HISAT2[126]. Protein predictions on the masked genomes were carried out with BRAKER2[127-134], using the mapped RNA-Seq reads and the Viridiplantae dataset from OrthoDB[135] as hints. Predicted proteins were then annotated with matches against Swiss-Prot, TrEMBL[30], NCBI NR[31] with BLASTp[136,137], and the Kyoto Encyclopedia of Genes and Genomes (KEGG)[34] with KofamKOALA[138], while protein domains were identified with InterProScan[139]. Gene ontology terms[37,38] were retrieved from the Swiss-Prot annotation and InterProScan results. MapMan[32,33] terms were retrieved with

bioRxiv preprint doi: https://doi.org/10.1101/2023.04.21.537482; this version posted April 23, 2023. The copyright holder for this preprint (which was not certified by peer review) is the author/funder, who has granted bioRxiv a license to display the preprint in perpetuity. It is made available under aCC-BY-NC-ND 4.0 International license.

Mercator[33,140]. The completeness of the annotations was assessed with BUSCO using the Eudicotyledons v.10 dataset. Genome annotations can be found in Supplementary Data Files 1 and 2.

Orthology and phylogenetic analyses

Groups of orthologous proteins were identified with OrthoMCL[36] for representative genomes of Brassicaceae: *Arabidopsis thaliana* (Araport11)[141,142] and *Brassica rapa* (FPSc v1.3)[143]; Amaranthaceae: *Beta vulgaris* (v1.2)[144], *Chenopodium quinoa* (v1)[145], *Salicornia bigelovii* (this study), *Salicornia europaea* (this study), and *Spinacia oleracea* (v1)[146]; Fabaceae: *Glycine max* (Wm82.a2.v1)[147] and *Phaseolus vulgaris* (v2.1)[148]; Solanaceae: *Solanum lycopersicum* (ITAG4.0)[149] and *Solanum melongena* (v3)[150]; and Poaceae *Sorghum bicolor* (v3.1.1)[151]. One isoform per gene was used for the analysis. All genome protein predictions were re-annotated by performing BLASTp[136,137] against the Swiss-Prot database[30]. Gene Ontology (GO) terms[37,38] were extracted from each best hit for each protein. Orthogroups shared across lists were identified with the Venn diagram creator of the University of Gent (http://bioinformatics.psb.ugent.be/webtools/Venn/). GO enrichment analyses on the orthogroup lists were analyzed with BINGO[152,153] using a Benjamini and Hochberg false discovery rate correction[154] of 0.05.

Family phylogenetic reconstruction was done by selecting BUSCO orthologs from the Eudicotyledons v10 dataset present in every species, resulting in a set of 1,377 proteins. Protein sequences were aligned with MUSCLE[155], informative sites were identified and retained with Gblocks[156], the alignments were concatenated and an

bioRxiv preprint doi: https://doi.org/10.1101/2023.04.21.537482; this version posted April 23, 2023. The copyright holder for this preprint (which was not certified by peer review) is the author/funder, who has granted bioRxiv a license to display the preprint in perpetuity. It is made available under aCC-BY-NC-ND 4.0 International license.

appropriate protein evolutionary model was identified with ModelTest-NG[157]. Phylogenetic analysis was done with maximum likelihood inference with RAxML-NG[49] under a JTT+I+G4 model and 1000 bootstrap replicates under the Transfer Bootstrap Expectation (TBE) method[50]. For the phylogenetic reconstruction of NHX proteins, Arabidopsis NHX protein sequences were searched in the genomes of all other species by BLAST, with a cutoff e-value of e-10. Only proteins longer than 200 aa were used for the analysis (Supplementary Data File 4). Protein sequences were aligned with MUSCLE and an appropriate protein evolutionary model was identified with ModelTest-NG. Phylogenetic analysis was done with maximum likelihood inference with RAxML-NG under a JTT+G4 model and 1000 bootstrap replicates under the Transfer Bootstrap Expectation (TBE) method.

Gene differential expression analysis

For gene differential expression analysis of *S. bigelovii* shoots, RNA-Seq reads were adapter trimmed with Trimmomatic v0.39[120] and quality checked with FastQC[121]. Transcript abundances were estimated with Salmon[158] and differentially expressed genes were identified with DESeq2[159] with a minimum of 10 counts and an adjusted p-value < 0.05. DE genes were clustered by hierarchical clustering of $\log_2$ transformed expression and displayed using MeV v.4.9[160]. GO enrichment analyses were done with BINGO[152,153] using a Benjamini and Hochberg false discovery rate correction[154] of 0.05. Overrepresentation of MapMan[32,33] bins were tested with Wilcoxon Rank Sum test and corrected for multiple testing with the Benjamini Hochberg correction with a *p*-value < 0.05.

bioRxiv preprint doi: https://doi.org/10.1101/2023.04.21.537482; this version posted April 23, 2023. The copyright holder for this preprint (which was not certified by peer review) is the author/funder, who has granted bioRxiv a license to display the preprint in perpetuity. It is made available under aCC-BY-NC-ND 4.0 International license.

Plant membrane extraction, fractionation, and protein quantitation

Membrane preparations were obtained for *S. bigelovii* shoots treated with 0, 50, 200, or 600 mM NaCl for 6 weeks with three biological replicates per treatment and processed similarly as described in Dunkley, et al. [57] with all steps done at 4 °C. 100 – 120 g of shoot tissue were blended in homogenization buffer (5% glycerol, 100 mM KCl, 0.5% PVP, 10 mM EDTA, 2 mM PMSF, 10% sucrose, 50 mM HEPES, pH 7.8) and osmotically adjusted with sucrose to shoot sap osmolality measured with a VAPRO® vapor pressure osmometer (ELITechGroup Biomedical Systems). The homogenate was filtered through three layers of cheesecloth and spun at 10,000 x *g* for 30 min to sediment debris and intact organelles. The supernatant containing the microsomal fraction was transferred to a new tube and spun at 100,000 x *g* for 1 h. The pellet was resuspended in 2 mL resuspension buffer (5% glycerol, 50 mM KCl, 10% sucrose, 25 mM HEPES, pH 7.8) and layered on top of a 24 mL continuous sucrose density gradient (20 – 45%). Gradients were spun at 100,000 x *g* for 14 h. Fractions were recovered each 2 mL with an Auto Densi-Flow II (Buchler Instruments) resulting in 12 different density fractions. Fraction density was measured with a digital refractometer (Brix/RI-Chek, Reichert). To release cytosolic proteins trapped inside microsomes, fractions were diluted 3 times in 160 mM Na_2CO_3, left on ice for 30 min, and spun at 100,000 x *g* for 1 h. The pellet was washed with 160 mM Na_2CO_3 and spun again at 100,000 x *g* for 1 h. The pellet was washed with water and spun at 100,000 x g for 1 h. The resultant pellet was resuspended in 1 mL of storage buffer (7 M urea, 2 M thiourea, 5 mM Tris-

bioRxiv preprint doi: https://doi.org/10.1101/2023.04.21.537482; this version posted April 23, 2023. The copyright holder for this preprint (which was not certified by peer review) is the author/funder, who has granted bioRxiv a license to display the preprint in perpetuity. It is made available under aCC-BY-NC-ND 4.0 International license.

HCl, pH 7.1) and stored at -80 °C. Protein concentrations were measured by the Bradford assay[161].

Protein digestion and LC-MS analyses

Proteins for each fraction were trypsin digested based on filter aided sample preparation[59]. 30 µg of protein were incubated with 100 mM DTT for 1 h at 37 °C. Samples were loaded into a Vivacon 500 hydrosart 30 kDa filter (Sartorius) and spun at 14,000 x *g* for 15 min. 100 µL of 50 mM iodoacetamide were added to the column, incubated for 20 min, and spun at 14,000 x *g* for 10 min. 100 µL of 8 M urea, 100 mM Tris-HCl, pH 7.8 were added and the sample was spun at 14,000 x *g* for 15 min. This step was repeated twice. 40 µL of trypsin 1:100 (Sequencing grade modified trypsin, Promega) in 50 mM ammonium bicarbonate were added to the sample and incubated in a wet chamber at 37 °C overnight. Samples were spun at 14,000 x *g* for 10 min. 100 µL of 50 mM ammonium bicarbonate were added to the column and spun at 14,000 x *g* for 15 min. 50 µL of 0.5 M NaCl were added to the column and spun at 14,000 x *g* for 15 min followed by the addition of 50 µL ammonium bicarbonate and another centrifugation step at 14,000 x *g* for 15 min. Filtered peptides were acidified by the addition of 2% trifluoroacetic acid (TFA) and desalted with Sep-Pak C18 cartridges (Waters Scientific). Samples were lyophilized, resuspended in 15 µL 3% acetonitrile 0.1% TFA, and quantified with Nanodrop measurement at 280 nm wavelength. 1 µg of peptides for label-free LC/MS analyses were loaded to an Ultimate 3000 UHPLC/Q-Exactive system (Thermo Scientific) with an Acclaim PepMap RSLC 75 µm × 15 cm nanoViper column and run for 1 h.

bioRxiv preprint doi: https://doi.org/10.1101/2023.04.21.537482; this version posted April 23, 2023. The copyright holder for this preprint (which was not certified by peer review) is the author/funder, who has granted bioRxiv a license to display the preprint in perpetuity. It is made available under aCC-BY-NC-ND 4.0 International license.

MS spectra analyses and protein abundance quantitation

Mass spectra peak files were compared against a combined set of *S. bigelovii* and *S. europaea* proteins derived from their genome annotation with MASCOT v. 2.4[162]. Database searching parameters included peptide tolerance of ± 10 ppm, fragment tolerance of ± 0.5 Da, carbamidomethyl modification, and reverse sequences as decoy. MASCOT files were loaded into SCAFFOLD 4[163] for protein quantitation and differential abundance analyses. For differential abundance analyses, MASCOT files were loaded as Multidimensional Protein Identification Technology (MudPIT) with three replicates per treatment. Protein identification required a 95% peptide identity and minimum of two assigned peptides per protein. Protein abundances were normalized by total spectrum counts. Differential protein abundances were tested at a significance of $p \leq 0.05$ and corrected for multiple testing with the Hochberg-Benjamini correction[154]. Differentially abundant proteins were analyzed for pathway and overrepresentation with MapMan[32,33,164] and GO enrichment analysis was performed with BINGO[152].

Subcellular localization prediction

Protein subcellular localization was predicted with the pRoloc[65-70] R package. To create a *Salicornia* organelle marker set, protein sequences of *S. bigelovii* and *S. europaea* genomes were combined. The *Salicornia* protein dataset was blasted against 279 Arabidopsis organelle markers retrieved from pRolocdata[57,60-64]. Positive hits with

bioRxiv preprint doi: https://doi.org/10.1101/2023.04.21.537482; this version posted April 23, 2023. The copyright holder for this preprint (which was not certified by peer review) is the author/funder, who has granted bioRxiv a license to display the preprint in perpetuity. It is made available under aCC-BY-NC-ND 4.0 International license.

Arabidopsis markers were *in silico* predicted for subcellular compartmentalization with mGOASVM Plant V2[165]. Proteins whose predicted subcellular localization by mGOASVM Plant V2 was congruent with their Arabidopsis organelle marker blast hit, were assigned as *Salicornia* organelle markers. To predict for protein subcellular localization based on protein abundance profiles in the 12 density fractions, protein abundances per fraction of samples coming from shoots of *S. bigelovii* plants treated with 0, 50, 200, and 600 mM NaCl were analyzed with pRoloc. pRoloc was run under a supervised maximum likelihood (ML) analysis with a support vector machines analysis with 1000 iterations and using the generated *Salicornia* organelle marker set as reference.

Validation of subcellular compartmentalization prediction of pRoloc by Western blot

The predicted subcellular localization by pRoloc was validated with western blots against organelle markers. 5 µg of protein per density fraction were separated in a 4-20% SDS-PAGE gel and used for western blot analyses using antibodies for different organelles (polyclonal antibodies generated in rabbit, Agrisera): Chloroplast PsbA (catalog number AS05 084) 1:10000 working dilution; Plasma membrane H^+ ATPase (catalog number AS07 260) 1:1000 working dilution; and Tonoplast V-ATPase (catalog number AS07 213) 1:2000 working dilution. Signal was detected by chemiluminescence using WesternBreeze® Chemiluminescent Kit anti-rabbit (Invitrogen) and according to the manufacturer's instructions. Western blot profiles for different subcellular localization marker proteins were compared against protein profiles generated with pRoloc.

bioRxiv preprint doi: https://doi.org/10.1101/2023.04.21.537482; this version posted April 23, 2023. The copyright holder for this preprint (which was not certified by peer review) is the author/funder, who has granted bioRxiv a license to display the preprint in perpetuity. It is made available under aCC-BY-NC-ND 4.0 International license.

RNA extraction and cloning of candidate genes into *E. coli*

RNA was extracted from shoots of *S. bigelovii* plants grown in 200 mM NaCl using TRIzol™ with an RNA MiniPrep kit (Zymo Research, USA), following the manufacturer's protocol. cDNA was prepared from the extracted, good quality RNA with SuperScript™ II (Invitrogen, USA), following the manufacturer's protocol. Genes were amplified by PCR using the high fidelity KOD DNA polymerase (Toyobo, Japan), cloned into pCR™8/GW/TOPO® (Invitrogen, USA), and transformed into *E. coli*. Since *S. bigelovii* is an autotetraploid undomesticated species, several isoforms per gene might be cloned. Entry clones were sequenced and compared with the reference transcriptome. Genes that did not match the sequence were re-amplified and cloned again. If the same polymorphisms were observed in subsequent amplifications, they were considered natural allelic variants and proceeded to further analysis. In the case two or more alleles were observed, alleles sharing equal sequences with *S. brachiata* or *S. europaea* were selected as it was assumed that conserved alleles across species would be more likely to be functional. Entry clones with and without stop codons per gene were recombined with Gateway™ LR Clonase™ II (Invitrogen, USA) into pAG426GAL-ccdB-EGFP. pAG426GAL-ccdB-EGFP was a gift from Susan Lindquist (Addgene plasmid # 14203).

Yeast transformation, spot assays, and subcellular localization

bioRxiv preprint doi: https://doi.org/10.1101/2023.04.21.537482; this version posted April 23, 2023. The copyright holder for this preprint (which was not certified by peer review) is the author/funder, who has granted bioRxiv a license to display the preprint in perpetuity. It is made available under aCC-BY-NC-ND 4.0 International license.

Plasmids were transformed into the salt sensitive AXT3 (Δena1-4::HIS3 Δnha1::LEU2 Δnhx1::TRP1) yeast strain by the lithium acetate method[166]. Yeast spot assays were carried out in synthetic defined (SD) medium: 1.7 g/L BD™ Difco™ yeast nitrogen base without amino acids and ammonium sulfate, 5 g/L ammonium sulfate, 0.77 g/L complete supplement mix (CSM) Drop-out – uracil (Formedium), adjusted to pH 5.6 with KOH, and supplemented with either 2% glucose or galactose; or in arginine phosphate (AP) medium[167]: 10 mM L-arginine, 8 mM phosphoric acid, 2 mM $MgSO_4$, 0.2 mM $CaCl_2$, 20 µg/L biotin, 2 mg/L calcium pantothenate, 2 µg/L folic acid, 400 µg/L niacin, 200 µg/L riboflavin, 10 mg/L inositol, 200 µg/L p-aminobenzoic acid, 400 µg/L $ZnSO_4$, 400 µg/L pyridoxine hydrochloride, 400 µg/L thiamine hydrochloride, 40 µg/L $CuSO_4$, 500 µg/L H_3BO_3, 100 µg/L KI, 200 µg/L $FeCl_3$, 200 µg/L Na_2MoO_4, 1mM KCl, 0.77 g/L complete supplement mix (CSM) Drop-out – uracil (Formedium), adjusted to pH 6.5 with L-arginine, and supplemented with either 2% glucose or galactose.

Yeast spot assays were done with three different colonies per construct. In short, to normalize growth, yeast transformed with pAG426GAL-gene-EGFP were grown in SD or AP medium with 2% glucose for two days at 30 °C. 200 µL of the pre-grown yeast were transferred into 1.8 mL of medium with 2% glucose and grown for 16 hours at 30 °C. The OD_{600} was measured and each sample was adjusted to an OD_{600} of 0.6 by diluting with medium without any carbon source. For each sample, four 10-fold dilutions were prepared. 10 µL per sample were spotted in each SD or AP plate. SD plates consisted in SD medium with 2% agar and supplemented with either 0, 100 mM, 150 mM, 175 mM, and 200 mM NaCl or 800 mM KCl. SD plates were supplemented with 2% galactose for all treatments and with 2% glucose for plates with 0 mM NaCl as

bioRxiv preprint doi: https://doi.org/10.1101/2023.04.21.537482; this version posted April 23, 2023. The copyright holder for this preprint (which was not certified by peer review) is the author/funder, who has granted bioRxiv a license to display the preprint in perpetuity. It is made available under aCC-BY-NC-ND 4.0 International license.

control. AP plates consisted of AP medium with 2% agar and supplemented with either 0, 20 mM, 30 mM, 40 mM, and 60 mM NaCl. AP plates were supplemented with 2% galactose for all treatments and with 2% glucose for plates with 0 mM NaCl as control. Plates were grown at 30 °C for 2 – 5 days. Subcellular localization of proteins was analyzed by EGFP fusions in the C' terminus of each protein and observed with a confocal laser scanning microscope (LSM 710, Zeiss, Germany). Images were acquired with Zen 2009 image software (Zess, Germany) and analyzed with Fiji image analysis software[168].

To assess the subcellular localization of SbiSALTY *in planta*, *SbiSALTY* was cloned into the pBWA(V)HS-GLosgfp vector and transfected into rice protoplasts as described in Zhang, et al. [169]. The ER-mCherry marker (TAIR: CD3-959)[170] and empty pBWA(V)HS-GLosgfp vector were used to confirm the subcellular localization of SbiSALTY.

Protein expression and purification

cDNA encoding SALTY was codon optimized (Integrated DNA Technologies, Inc.), subcloned into the Expresso® SUMO Cloning system, a modified PET32a vector with an N-terminal His_6-SUMO expression tag and SUMO protease cleavage site (Lucigen Corporation). SALTY fusion was expressed in Codon+ BL21 (DE3) *E. coli* cells from Merck (Cat# CMC0014). Cells were grown in Luria broth or labeled M9 medium with kanamycin (His_6-SUMO-SALTY). The pre-culture and unlabeled cell growth were accomplished using the auto-induction method[171]. The cell culture media were grown and suspended until OD=0.6, then induced with 0.5 mM IPTG and incubated at 25°C for 24h.

bioRxiv preprint doi: https://doi.org/10.1101/2023.04.21.537482; this version posted April 23, 2023. The copyright holder for this preprint (which was not certified by peer review) is the author/funder, who has granted bioRxiv a license to display the preprint in perpetuity. It is made available under aCC-BY-NC-ND 4.0 International license.

Cells were collected and resuspended in 50 mL lysis buffer (50 mM Tris-HCl, pH 7.5, 250 mM NaCl, 30 mM Imidazole, 1 mM TCEP for His_6-tag recombinant proteins) per liter of culture. 0.5 mM phenylmethylsulfonyl fluoride (PMSF) and 1 mM β-mercaptoethanol (β-ME) were added to the lysis buffer. Cells were lysed using a cell disruptor (Constant Systems) and DNase I and RNase A (Invitrogen, Cat# 12091039 and AM2224) were added to digest the DNA/RNA. After centrifugation, the clarified lysate was applied to a HisTrap HP (GE Healthcare) and eluted with elution buffer (Lysis Buffer + 0.5 M Imidazole). To remove the His_6-SUMO tag, the protein was cleaved with SUMO protease (Invitrogen, Cat# 12588018), and purified using an AKTA with a HisTrap HP column. The uniform ^{15}N-labeling of recombinant protein was done according to well-established protocols[172].

Sequence analysis and circular dichroism spectroscopy

In silico prediction for intrinsically disorder domains of SbiSALTY protein was done with DisEMBL v.1.5[173]. Coiled-coils region prediction was done with COILS[174]. The circular dichroism (CD) spectra of SALTY (10 μM in 50mM MES, 50mM NaCl, pH 6.5) were acquired using a Jasco 1500 spectropolarimeter flushed with N_2 and a cuvette with 0.1 cm path length. The spectra to investigate its secondary and tertiary structure were measured from 190 to 260 nm and 250 to 350 nm with 0.2 nm intervals. The temperature stability was assessed with temperatures ranging from 25 – 90°C at three wavelengths, 201, 208 and 222 nm. The spectrum of the buffer was subtracted. The internal software and CAPITO (CD Analysis and Plotting Tool) were used to assess the secondary structure elements of fused SALTY based on its CD spectrum[175].

bioRxiv preprint doi: https://doi.org/10.1101/2023.04.21.537482; this version posted April 23, 2023. The copyright holder for this preprint (which was not certified by peer review) is the author/funder, who has granted bioRxiv a license to display the preprint in perpetuity. It is made available under aCC-BY-NC-ND 4.0 International license.

Protein NMR experiments

The NMR samples of ^{15}N-SALTY$_{1-357}$ contained 50-1000 µM protein in NMR buffer (50 mM MES, 50 mM NaCl, pH 6.5, 1 mM TCEP and 5%/95% D_2O/H_2O *v*/*v*). All NMR spectra were acquired at 5℃ on an 800 MHz Bruker Advance NEO spectrometer equipped with TCI ^{1}H&^{19}F/^{13}C/^{15}N cryogenic probe head, running Topspin version 4.0.7.

Acknowledgements

Research reported in this publication was supported by the King Abdullah University of Science and Technology (KAUST). We thank E. Glenn at University of Arizona and M. Sagi at Blaustein Institute for Desert Research for their assistance in providing seeds. We also thank E. Martinoia at University of Zurich for his technical advice on gradient formation for membrane separation. We would like to thank our visiting student, J. Otero, for his assistance in the laboratory.

Contributions

M.T., N.V.F., O.R.S., and S.M.S. conceived the project and experiments. M.T. and S.M.S. supervised the research. O.R.S. and V.J.M. generated the sequencing data. D.B., E.H., and J.C. performed the karyotyping and flow cytometry. O.R.S. performed the bioinformatic analyses and genome assemblies. O.R.S. performed the phenotypic, transcriptomic, and proteomic experiments and analyses. M.P.R., O.R.S., and V.J.M overlooked the plant material. L.J., and M.J. led the protein structural analyses. K.C.

bioRxiv preprint doi: https://doi.org/10.1101/2023.04.21.537482; this version posted April 23, 2023. The copyright holder for this preprint (which was not certified by peer review) is the author/funder, who has granted bioRxiv a license to display the preprint in perpetuity. It is made available under aCC-BY-NC-ND 4.0 International license.

and O.R.S. did protein production and purification. K.C., L.J., and M.J. performed the NMR and CDD analyses. K.C. performed the rice protoplast transformation. All authors contributed to the writing of the manuscript. M.T., O.R.S., and S.M.S. organized the manuscript.

Competing interests

The authors declare no competing interests

Data availability

All sequencing data are available in the NCBI Short Read Archive (SRA), Bioprojects PRJNA733891, and PRJNA733892. Genome assemblies and annotation data can be found at www.salicorniadb.org .

bioRxiv preprint doi: https://doi.org/10.1101/2023.04.21.537482; this version posted April 23, 2023. The copyright holder for this preprint (which was not certified by peer review) is the author/funder, who has granted bioRxiv a license to display the preprint in perpetuity. It is made available under aCC-BY-NC-ND 4.0 International license.

References

1. Munns, R. & Tester, M. Mechanisms of salinity tolerance. *Annual Review of Plant Biology* **59**, 651-681 (2008).
2. FAO & ITPS. *Status of the World's Soil Resources (SWR) - Main Report*, (Food and Agriculture Organization of the United Nations and Intergovernmental Technical Panel on Soils, Rome, Italy, 2015).
3. Ivushkin, K. *et al.* Global mapping of soil salinity change. *Remote Sensing of Environment* **231**(2019).
4. FAO. Global Soil Partnership. http://www.fao.org/global-soil-partnership/areas-of-work/soil-salinity/en/ (2021).
5. UN. *World Population Prospects 2019: Highlights*, (United Nations, Department of Economic and Social Affairs, Population Division, 2019).
6. Kadereit, G. *et al.* A taxonomic nightmare comes true: Phylogeny and biogeography of glassworts (*Salicornia L., Chenopodiaceae*). *Taxon* **56**, 1143-1170 (2007).
7. Lv, S. *et al.* Multiple compartmentalization of sodium conferred salt tolerance in *Salicornia europaea*. *Plant Physiol Biochem* **51**(2012).
8. Ventura, Y. & Sagi, M. Halophyte crop cultivation: The case for Salicornia and Sarcocornia. *Environmental and Experimental Botany* **92**, 144-153 (2013).
9. Reddy, M.P., Sanish, S. & Iyengar, E.R.R. Compartmentation of ions and organic compounds in *Salicornia brachiata* Roxb. *Biologia Plantarum* **35**, 547 (1993).
10. Ayala, F. & Oleary, J.W. Growth and physiology of *Salicornia bigelovii* Torr at suboptimal salinity. *International Journal of Plant Sciences* **156**, 197-205 (1995).
11. Ayala, F., OLeary, J.W. & Schumaker, K.S. Increased vacuolar and plasma membrane H^+-ATPase activities in *Salicornia bigelovii* Torr in response to NaCl. *Journal of Experimental Botany* **47**, 25-32 (1996).
12. Parks, G.E., Dietrich, M.A. & Schumaker, K.S. Increased vacuolar Na^+/H^+ exchange activity in *Salicornia bigelovii* Torr. in response to NaCl. *Journal of Experimental Botany* **53**, 1055-1065 (2002).
13. Flowers, T.J. & Yeo, A.R. Ion Relations of Plants under Drought and Salinity. *Australian Journal of Plant Physiology* **13**, 75-91 (1986).
14. Glenn, E.P., Brown, J.J. & Blumwald, E. Salt tolerance and crop potential of halophytes. *Crit Rev Plant Sci* **18**(1999).
15. Webb, K.L. NaCl effects on growth and transpiration in *Salicornia bigelovii* a salt-marsh halophyte. *Plant and Soil* **24**, 261-268 (1966).
16. Brown, J.J., Glenn, E.P., Fitzsimmons, K.M. & Smith, S.E. Halophytes for the treatment of saline aquaculture effluent. *Aquaculture* **175**, 255-268 (1999).
17. Ohori, T. & Fujiyama, H. Water deficit and abscisic acid production of *Salicornia bigelovii* under salinity stress. *Soil Science and Plant Nutrition* **57**, 566-572 (2011).
18. Kong, Y. & Zheng, Y.B. Potential of Producing Salicornia bigelovii Hydroponically as a Vegetable at Moderate NaCl Salinity. *Hortscience* **49**, 1154-1157 (2014).
19. Roy, S.J., Negrão, S. & Tester, M. Salt resistant crop plants. *Current Opinion in Biotechnology* **26**, 115-124 (2014).
20. Isayenkov, S.V. & Maathuis, F.J.M. Plant Salinity Stress: Many Unanswered Questions Remain. *Frontiers in Plant Science* **10**(2019).

bioRxiv preprint doi: https://doi.org/10.1101/2023.04.21.537482; this version posted April 23, 2023. The copyright holder for this preprint (which was not certified by peer review) is the author/funder, who has granted bioRxiv a license to display the preprint in perpetuity. It is made available under aCC-BY-NC-ND 4.0 International license.

21. Maathuis, F.J.M. & Amtmann, A. K $^{+}$ Nutrition and Na $^{+}$ Toxicity: The Basis of Cellular K $^{+}$ /Na $^{+}$ Ratios. *Annals of Botany* **84**, 123-133 (1999).
22. Davenport, R.J. & Tester, M. A weakly voltage-dependent, nonselective cation channel mediates toxic sodium influx in wheat. *Plant Physiology* **122**, 823-834 (2000).
23. Demidchik, V. & Tester, M. Sodium fluxes through nonselective cation channels in the plasma membrane of protoplasts from Arabidopsis roots. *Plant Physiology* **128**, 379-387 (2002).
24. Benito, B., Haro, R., Amtmann, A., Cuin, T.A. & Dreyer, I. The twins K+ and Na+ in plants. *Journal of Plant Physiology* **171**, 723-731 (2014).
25. Flowers, T.J., Galal, H.K. & Bromham, L. Evolution of halophytes: multiple origins of salt tolerance in land plants. *Functional Plant Biology* **37**, 604-612 (2010).
26. Jefferies, R.L., Davy, A.J. & Rudmik, T. Population Biology of the Salt Marsh Annual *Salicornia Europaea* agg. *Journal of Ecology* **69**, 17-31 (1981).
27. Sun, H.Q., Ding, J., Piednoel, M. & Schneeberger, K. findGSE: estimating genome size variation within human and Arabidopsis using k-mer frequencies. *Bioinformatics* **34**, 550-557 (2018).
28. Rhie, A., Walenz, B.P., Koren, S. & Phillippy, A.M. Merqury: reference-free quality, completeness, and phasing assessment for genome assemblies. *Genome Biology* **21**(2020).
29. Kaligarič, M., Bohanec, B., Simonovik, B. & Šajna, N. Genetic and morphologic variability of annual glassworts (Salicornia L.) from the Gulf of Trieste (Northern Adriatic). *Aquatic Botany* **89**, 275-282 (2008).
30. Bateman, A. *et al.* UniProt: a worldwide hub of protein knowledge. *Nucleic Acids Research* **47**, D506-D515 (2019).
31. Coordinators, N.R. Database resources of the National Center for Biotechnology Information. *Nucleic acids research* **44**, D7-D19 (2016).
32. Thimm, O. *et al.* mapman: a user-driven tool to display genomics data sets onto diagrams of metabolic pathways and other biological processes. *The Plant Journal* **37**, 914-939 (2004).
33. Schwacke, R. *et al.* MapMan4: A Refined Protein Classification and Annotation Framework Applicable to Multi-Omics Data Analysis. *Molecular Plant* **12**, 879-892 (2019).
34. Kanehisa, M. & Goto, S. KEGG: Kyoto Encyclopedia of Genes and Genomes. *Nucleic Acids Research* **28**, 27-30 (2000).
35. Simao, F.A., Waterhouse, R.M., Ioannidis, P., Kriventseva, E.V. & Zdobnov, E.M. BUSCO: assessing genome assembly and annotation completeness with single-copy orthologs. *Bioinformatics* **31**, 3210-3212 (2015).
36. Li, L., Stoeckert, C.J. & Roos, D.S. OrthoMCL: Identification of ortholog groups for eukaryotic genomes. *Genome Research* **13**, 2178-2189 (2003).
37. Carbon, S. *et al.* The Gene Ontology Resource: 20 years and still GOing strong. *Nucleic Acids Research* **47**, D330-D338 (2019).
38. Ashburner, M. *et al.* Gene Ontology: tool for the unification of biology. *Nature Genetics* **25**, 25-29 (2000).
39. Choi, W.-G., Toyota, M., Kim, S.-H., Hilleary, R. & Gilroy, S. Salt stress-induced Ca^{2}+ waves are associated with rapid, long-distance root-to-shoot signaling in plants. *Proceedings of the National Academy of Sciences* **111**, 6497-6502 (2014).
40. Schmöckel, S.M. *et al.* Different NaCl-Induced Calcium Signatures in the Arabidopsis thaliana Ecotypes Col-0 and C24. *PLOS ONE* **10**, e0117564 (2015).
41. Manishankar, P., Wang, N., Koster, P., Alatar, A.A. & Kudla, J. Calcium Signaling during Salt Stress and in the Regulation of Ion Homeostasis. *J Exp Bot* (2018).
42. Apse, M.P., Aharon, G.S., Snedden, W.A. & Blumwald, E. Salt tolerance conferred by overexpression of a vacuolar Na^{+}/H^{+} antiport in Arabidopsis. *Science* **285**, 1256-1258 (1999).

bioRxiv preprint doi: https://doi.org/10.1101/2023.04.21.537482; this version posted April 23, 2023. The copyright holder for this preprint (which was not certified by peer review) is the author/funder, who has granted bioRxiv a license to display the preprint in perpetuity. It is made available under aCC-BY-NC-ND 4.0 International license.

43. Yokoi, S. *et al.* Differential expression and function of *Arabidopsis thaliana* NHX Na^+/H^+ antiporters in the salt stress response. *The Plant Journal* **30**, 529-539 (2002).
44. Pardo, J.M., Cubero, B., Leidi, E.O. & Quintero, F.J. Alkali cation exchangers: roles in cellular homeostasis and stress tolerance. *Journal of Experimental Botany* **57**, 1181-1199 (2006).
45. Bassil, E. *et al.* The Arabidopsis intracellular Na^+/H^+ antiporters NHX5 and NHX6 are endosome associated and necessary for plant growth and development. *The Plant Cell Online* **23**, 224-239 (2011).
46. Shi, H., Ishitani, M., Kim, C. & Zhu, J.-K. The Arabidopsis thaliana salt tolerance gene *SOS1* encodes a putative Na^+/H^+ antiporter. *Proceedings of the National Academy of Sciences* **97**, 6896-6901 (2000).
47. An, R. *et al.* AtNHX8, a member of the monovalent cation:proton antiporter-1 family in *Arabidopsis thaliana*, encodes a putative Li^+/H^+ antiporter. *The Plant Journal* **49**, 718-728 (2007).
48. Wu, G.Q., Wang, J.L. & Li, S.J. Genome-Wide Identification of Na+/H+ Antiporter (NHX) Genes in Sugar Beet (Beta vulgaris L.) and Their Regulated Expression under Salt Stress. *Genes* **10**(2019).
49. Kozlov, A.M., Darriba, D., Flouri, T., Morel, B. & Stamatakis, A. RAxML-NG: a fast, scalable and user-friendly tool for maximum likelihood phylogenetic inference. *Bioinformatics* **35**, 4453-4455 (2019).
50. Lemoine, F. *et al.* Renewing Felsenstein's phylogenetic bootstrap in the era of big data. *Nature* **556**, 452-+ (2018).
51. Zhang, L. *et al.* Identification of an Apoplastic Protein Involved in the Initial Phase of Salt Stress Response in Rice Root by Two-Dimensional Electrophoresis. *Plant Physiology* **149**, 916-928 (2009).
52. Sunarpi *et al.* Enhanced salt tolerance mediated by AtHKT1 transporter-induced Na^+ unloading from xylem vessels to xylem parenchyma cells. *The Plant Journal* **44**, 928-938 (2005).
53. Davenport, R.J. *et al.* The Na^+ transporter AtHKT1;1 controls retrieval of Na^+ from the xylem in Arabidopsis. *Plant, Cell & Environment* **30**, 497-507 (2007).
54. Katschnig, D., Bliek, T., Rozema, J. & Schat, H. Constitutive high-level *SOS1* expression and absence of *HKT1;1* expression in the salt-accumulating halophyte *Salicornia dolichostachya*. *Plant Science* **234**, 144-154 (2015).
55. Hodges, T.K., Leonard, R.T., Keenan, T.W. & Bracker, C.E. Purification of an Ion-Stimulated Adenosine-Triphosphatase from Plant Roots - Association with Plasma-Membranes. *Proceedings of the National Academy of Sciences of the United States of America* **69**, 3307-& (1972).
56. Yang, H. & Murphy, A. Membrane Preparation, Sucrose Density Gradients and Two-phase Separation Fractionation from Five-day-old *Arabidopsis* seedlings. *Bio-protocol* **3**(2013).
57. Dunkley, T.P.J. *et al.* Mapping the Arabidopsis organelle proteome. *Proceedings of the National Academy of Sciences of the United States of America* **103**, 6518-6523 (2006).
58. Sadowski, P.G. *et al.* Quantitative proteomic approach to study subcellular localization of membrane proteins. *Nat. Protocols* **1**, 1778-1789 (2006).
59. Wisniewski, J.R., Zougman, A., Nagaraj, N. & Mann, M. Universal sample preparation method for proteome analysis. *Nature Methods* **6**, 359-U60 (2009).
60. Ferro, M. *et al.* AT_CHLORO, a Comprehensive Chloroplast Proteome Database with Subplastidial Localization and Curated Information on Envelope Proteins. *Molecular & Cellular Proteomics* **9**, 1063-1084 (2010).
61. Trotter, M.W.B., Sadowski, P.G., Dunkley, T.P.J., Groen, A.J. & Lilley, K.S. Improved sub-cellular resolution via simultaneous analysis of organelle proteomics data across varied experimental conditions. *Proteomics* **10**, 4213-4219 (2010).
62. Nikolovski, N. *et al.* Putative Glycosyltransferases and Other Plant Golgi Apparatus Proteins Are Revealed by LOPIT Proteomics. *Plant Physiology* **160**, 1037-1051 (2012).

bioRxiv preprint doi: https://doi.org/10.1101/2023.04.21.537482; this version posted April 23, 2023. The copyright holder for this preprint (which was not certified by peer review) is the author/funder, who has granted bioRxiv a license to display the preprint in perpetuity. It is made available under aCC-BY-NC-ND 4.0 International license.

63. Groen, A.J. *et al.* Identification of Trans-Golgi Network Proteins in Arabidopsis thaliana Root Tissue. *Journal of Proteome Research* **13**, 763-776 (2014).
64. Nikolovski, N., Shliaha, P.V., Gatto, L., Dupree, P. & Lilley, K.S. Label-Free Protein Quantification for Plant Golgi Protein Localization and Abundance. *Plant Physiology* **166**, 1033-1043 (2014).
65. Gatto, L., Breckels, L.M., Wieczorek, S., Burger, T. & Lilley, K.S. Mass-spectrometry-based spatial proteomics data analysis using pRoloc and pRolocdata. *Bioinformatics* **30**, 1322-4 (2014).
66. Breckels, L.M. *et al.* The effect of organelle discovery upon sub-cellular protein localisation. *Journal of Proteomics* **88**, 129-140 (2013).
67. Gatto, L. *et al.* A Foundation for Reliable Spatial Proteomics Data Analysis. *Molecular & Cellular Proteomics* **13**, 1937-1952 (2014).
68. Breckels, L.M. *et al.* Learning from Heterogeneous Data Sources: An Application in Spatial Proteomics. *PLoS Comput Biol* **12**, e1004920 (2016).
69. Breckels, L.M., Mulvey, C.M., Lilley, K.S. & Gatto, L. A Bioconductor workflow for processing and analysing spatial proteomics data. *F1000Res* **5**, 2926 (2016).
70. Crook, O.M., Breckels, L.M., Lilley, K.S., Kirk, P.D.W. & Gatto, L. A Bioconductor workflow for the Bayesian analysis of spatial proteomics. *F1000Res* **8**, 446 (2019).
71. Wu, S.J., Ding, L. & Zhu, J.K. SOS1, a genetic locus essential for salt tolerance and potassium acquisition. *Plant Cell* **8**, 617-627 (1996).
72. Qiu, Q.S., Guo, Y., Dietrich, M.A., Schumaker, K.S. & Zhu, J.K. Regulation of SOS1, a plasma membrane Na+/H+ exchanger in Arabidopsis thaliana, by SOS2 and SOS3. *Proceedings of the National Academy of Sciences of the United States of America* **99**, 8436-8441 (2002).
73. Qiu, Q.S., Barkla, B.J., Vera-Estrella, R., Zhu, J.K. & Schumaker, K.S. Na^+/H^+ exchange activity in the plasma membrane of Arabidopsis. *Plant Physiology* **132**, 1041-1052 (2003).
74. Shi, H., Quintero, F.J., Pardo, J.M. & Zhu, J.-K. The putative plasma membrane Na^+/H^+ antiporter SOS1 controls long-distance Na^+ transport in plants. *The Plant Cell Online* **14**, 465-477 (2002).
75. Yadav, N.S., Shukla, P.S., Jha, A., Agarwal, P.K. & Jha, B. The SbSOS1 gene from the extreme halophyte Salicornia brachiata enhances Na(+) loading in xylem and confers salt tolerance in transgenic tobacco. *BMC Plant Biol* **12**, 188 (2012).
76. Quintero, F.J., Blatt, M.R. & Pardo, J.M. Functional conservation between yeast and plant endosomal Na^+/H^+ antiporters. *FEBS Letters* **471**, 224-228 (2000).
77. Barragan, V. *et al.* Ion exchangers NHX1 and NHX2 mediate active potassium uptake into vacuoles to regulate cell turgor and stomatal function in Arabidopsis. *Plant Cell* **24**, 1127-1142 (2012).
78. Leidi, E.O. *et al.* The AtNHX1 exchanger mediates potassium compartmentation in vacuoles of transgenic tomato. *The Plant Journal* **61**, 495-506 (2010).
79. Bassil, E. *et al.* The Arabidopsis Na+/H+ Antiporters NHX1 and NHX2 Control Vacuolar pH and K+ Homeostasis to Regulate Growth, Flower Development, and Reproduction. *Plant Cell* **23**, 3482-3497 (2011).
80. Bassil, E., Zhang, S.Q., Gong, H.J., Tajima, H. & Blumwald, E. Cation Specificity of Vacuolar NHX-Type Cation/H+ Antiporters. *Plant Physiology* **179**, 616-629 (2019).
81. Osawa, H., Stacey, G. & Gassmann, W. ScOPT1 and AtOPT4 function as proton-coupled oligopeptide transporters with broad but distinct substrate specificities. *Biochemical Journal* **393**, 267 (2005).
82. Wormit, A., Traub, M., FlöRchinger, M., Neuhaus, H E. & MöHlmann, T. Characterization of three novel members of the Arabidopsis thaliana equilibrative nucleoside transporter (ENT) family. *Biochemical Journal* **383**, 19-26 (2004).
83. Bernard, C. *et al.* Equilibrative nucleoside transporter 1 (ENT1) is critical for pollen germination and vegetative growth in Arabidopsis. *Journal of Experimental Botany* **62**, 4627-4637 (2011).

bioRxiv preprint doi: https://doi.org/10.1101/2023.04.21.537482; this version posted April 23, 2023. The copyright holder for this preprint (which was not certified by peer review) is the author/funder, who has granted bioRxiv a license to display the preprint in perpetuity. It is made available under aCC-BY-NC-ND 4.0 International license.

84. Wright, E.M. Glucose transport families SLC5 and SLC50. *Molecular Aspects of Medicine* **34**, 183-196 (2013).
85. Bala, P.A., Foster, J., Carvelli, L. & Henry, L.K. SLC6 Transporters: Structure, Function, Regulation, Disease Association and Therapeutics. *Molecular aspects of medicine* **34**, 197-219 (2013).
86. Alqahtani, M. *et al.* The role of PQL genes in response to salinity tolerance in Arabidopsis and barley. *Plant Direct* **5**(2021).
87. Kawano-Kawada, M. *et al.* A PQ-loop protein Ypq2 is involved in the exchange of arginine and histidine across the vacuolar membrane of Saccharomyces cerevisiae. *Scientific Reports* **9**(2019).
88. Kalatzis, V., Cherqui, S., Antignac, C. & Gasnier, B. Cystinosin, the protein defective in cystinosis, is a H^+-driven lysosomal cystine transporter. *The EMBO Journal* **20**, 5940 (2001).
89. Jézégou, A. *et al.* Heptahelical protein PQLC2 is a lysosomal cationic amino acid exporter underlying the action of cysteamine in cystinosis therapy. *Proceedings of the National Academy of Sciences* **109**, E3434–E3443 (2012).
90. Greenfield, N.J. Using circular dichroism spectra to estimate protein secondary structure. *Nature Protocols* **1**, 2876-2890 (2006).
91. Chemes, L.B., Alonso, L.G., Noval, M.G. & de Prat-Gay, G. Circular dichroism techniques for the analysis of intrinsically disordered proteins and domains. *Methods Mol Biol* **895**, 387-404 (2012).
92. Konrat, R. NMR contributions to structural dynamics studies of intrinsically disordered proteins. *Journal of Magnetic Resonance* **241**, 74-85 (2014).
93. Solyom, Z. *et al.* BEST-TROSY experiments for time-efficient sequential resonance assignment of large disordered proteins. *Journal of Biomolecular Nmr* **55**, 311-321 (2013).
94. Ambrosone, A. *et al.* The Arabidopsis RNA-Binding Protein AtRGGA Regulates Tolerance to Salt and Drought Stress. *Plant Physiology* **168**, 292 (2015).
95. Jones, R.L. The Isolation of Endoplasmic-Reticulum from Barley Aleurone Layers. *Planta* **150**, 58-69 (1980).
96. Schaller, G.E. Isolation of Endoplasmic Reticulum and Its Membrane. *Methods Mol Biol* **1511**, 119-129 (2017).
97. Kelley, L.A., Mezulis, S., Yates, C.M., Wass, M.N. & Sternberg, M.J.E. The Phyre2 web portal for protein modeling, prediction and analysis. *Nature Protocols* **10**, 845-858 (2015).
98. Lv, S. *et al.* Sodium plays a more important role than potassium and chloride in growth of Salicornia europaea. *Acta Physiologiae Plantarum* **34**, 503-513 (2012).
99. Sze, H. H^+-translocating ATPases of the plasma membrane and tonoplast of plant cells. *Physiologia Plantarum* **61**, 683-691 (1984).
100. Yamaguchi, T., Apse, M.P., Shi, H. & Blumwald, E. Topological analysis of a plant vacuolar Na^+/H^+ antiporter reveals a luminal C terminus that regulates antiporter cation selectivity. *Proceedings of the National Academy of Sciences* **100**, 12510-12515 (2003).
101. Yamaguchi, T., Aharon, G.S., Sottosanto, J.B. & Blumwald, E. Vacuolar Na^+/H^+ antiporter cation selectivity is regulated by calmodulin from within the vacuole in a Ca^{2+} and pH dependent manner. *Proceedings of the National Academy of Sciences of the United States of America* **102**, 16107-16112 (2005).
102. Møller, I.S. *et al.* Shoot Na+ exclusion and increased salinity tolerance engineered by cell type-specific alteration of Na+ transport in Arabidopsis. *Plant Cell* **21**(2009).
103. Kiledjian, M. & Dreyfuss, G. Primary Structure and Binding-Activity of the Hnrnp U-Protein - Binding Rna through Rgg Box. *Embo Journal* **11**, 2655-2664 (1992).
104. Castello, A. *et al.* Insights into RNA Biology from an Atlas of Mammalian mRNA-Binding Proteins. *Cell* **149**, 1393-1406 (2012).
105. Thandapani, P., O'Connor, T.R., Bailey, T.L. & Richard, S. Defining the RGG/RG Motif. *Molecular Cell* **50**, 613-623 (2013).

bioRxiv preprint doi: https://doi.org/10.1101/2023.04.21.537482; this version posted April 23, 2023. The copyright holder for this preprint (which was not certified by peer review) is the author/funder, who has granted bioRxiv a license to display the preprint in perpetuity. It is made available under aCC-BY-NC-ND 4.0 International license.

106. Dure, L., 3rd. A repeating 11-mer amino acid motif and plant desiccation. *Plant J* **3**, 363-9 (1993).
107. Garay-Arroyo, A., Colmenero-Flores, J.M., Garciarrubio, A. & Covarrubias, A.A. Highly hydrophilic proteins in prokaryotes and eukaryotes are common during conditions of water deficit. *Journal of Biological Chemistry* **275**, 5668-5674 (2000).
108. Battaglia, M., Olvera-Carrillo, Y., Garciarrubio, A., Campos, F. & Covarrubias, A.A. The enigmatic LEA proteins and other hydrophilins. *Plant Physiology* **148**, 6-24 (2008).
109. Uversky, V.N. Intrinsically disordered proteins in overcrowded milieu: Membrane-less organelles, phase separation, and intrinsic disorder. *Current Opinion in Structural Biology* **44**, 18-30 (2017).
110. Cuevas-Velazquez, C.L. & Dinneny, J.R. Organization out of disorder: liquid-liquid phase separation in plants. *Curr Opin Plant Biol* **45**, 68-74 (2018).
111. Wallmann, A. & Kesten, C. Common Functions of Disordered Proteins across Evolutionary Distant Organisms. *International Journal of Molecular Sciences* **21**(2020).
112. Mitrea, D.M. & Kriwacki, R.W. Phase separation in biology; functional organization of a higher order. *Cell Communication and Signaling* **14**(2016).
113. Buchan, J.R. mRNP granules Assembly, function, and connections with disease. *Rna Biology* **11**, 1019-1030 (2014).
114. Anderson, P. & Kedersha, N. Stress granules: The Tao of RNA triage. *Trends in Biochemical Sciences* **33**, 141-150 (2008).
115. Jain, S. & Parker, R. The Discovery and Analysis of P Bodies. *Ten Years of Progress in Gw/P Body Research* **768**, 23-43 (2013).
116. R-Core_Team. R: A Language and Environment for Statistical Computing. https://www.R-project.org/ (Vienna, Austria, 2020).
117. Kato, A., Lamb, J.C. & Birchler, J.A. Chromosome painting using repetitive DNA sequences as probes for somatic chromosome identification in maize. *Proceedings of the National Academy of Sciences of the United States of America* **101**, 13554-13559 (2004).
118. Doležel, J., Greilhuber, J. & Suda, J. Estimation of nuclear DNA content in plants using flow cytometry. *Nature Protocols* **2**, 2233-2244 (2007).
119. Marcais, G. & Kingsford, C. A fast, lock-free approach for efficient parallel counting of occurrences of k-mers. *Bioinformatics* **27**, 764-770 (2011).
120. Bolger, A.M., Lohse, M. & Usadel, B. Trimmomatic: a flexible trimmer for Illumina sequence data. *Bioinformatics* **30**, 2114-2120 (2014).
121. Andrews, S. FastQC: a quality control tool for high throughput sequence data. Available online at: http://www.bioinformatics.babraham.ac.uk/projects/fastqc/. (2010).
122. Cheng, H.Y., Concepcion, G.T., Feng, X.W., Zhang, H.W. & Li, H. Haplotype-resolved de novo assembly using phased assembly graphs with hifiasm. *Nature Methods* **18**, 170-+ (2021).
123. Smit, A., Hubley, R. & Green, P. RepeatMasker Open-4.0 <http://www.repeatmasker.org>. (2013-2015).
124. Hubley, R. *et al.* The Dfam database of repetitive DNA families. *Nucleic Acids Research* **44**, D81-D89 (2016).
125. Bao, W.D., Kojima, K.K. & Kohany, O. Repbase Update, a database of repetitive elements in eukaryotic genomes. *Mobile DNA* **6** 11 (2015).
126. Kim, D., Paggi, J.M., Park, C., Bennett, C. & Salzberg, S.L. Graph-based genome alignment and genotyping with HISAT2 and HISAT-genotype. *Nature Biotechnology* **37**, 907-915 (2019).
127. Bruna, T., Hoff, K.J., Lomsadze, A., Stanke, M. & Borodovsky, M. BRAKER2: automatic eukaryotic genome annotation with GeneMark-EP+ and AUGUSTUS supported by a protein database. *NAR Genom Bioinform* **3**, lqaa108 (2021).

bioRxiv preprint doi: https://doi.org/10.1101/2023.04.21.537482; this version posted April 23, 2023. The copyright holder for this preprint (which was not certified by peer review) is the author/funder, who has granted bioRxiv a license to display the preprint in perpetuity. It is made available under aCC-BY-NC-ND 4.0 International license.

128. Hoff, K.J., Lomsadze, A., Borodovsky, M. & Stanke, M. Whole-Genome Annotation with BRAKER. *Methods in molecular biology* **1962**, 65-95 (2019).
129. Bruna, T., Lomsadze, A. & Borodovsky, M. GeneMark-EP+: eukaryotic gene prediction with self-training in the space of genes and proteins. *NAR Genom Bioinform* **2**, lqaa026 (2020).
130. Lomsadze, A., Ter-Hovhannisyan, V., Chernoff, Y.O. & Borodovsky, M. Gene identification in novel eukaryotic genomes by self-training algorithm. *Nucleic Acids Research* **33**, 6494-6506 (2005).
131. Buchfink, B., Xie, C. & Huson, D.H. Fast and sensitive protein alignment using DIAMOND. *Nat Methods* **12**, 59-60 (2015).
132. Iwata, H. & Gotoh, O. Benchmarking spliced alignment programs including Spaln2, an extended version of Spaln that incorporates additional species-specific features. *Nucleic Acids Research* **40**(2012).
133. Lomsadze, A., Burns, P.D. & Borodovsky, M. Integration of mapped RNA-Seq reads into automatic training of eukaryotic gene finding algorithm. *Nucleic Acids Research* **42**, e119-e119 (2014).
134. Stanke, M., Schoffmann, O., Morgenstern, B. & Waack, S. Gene prediction in eukaryotes with a generalized hidden Markov model that uses hints from external sources. *Bmc Bioinformatics* **7**, 62 (2006).
135. Kriventseva, E.V. *et al.* OrthoDB v10: sampling the diversity of animal, plant, fungal, protist, bacterial and viral genomes for evolutionary and functional annotations of orthologs. *Nucleic Acids Research* **47**, D807-D811 (2019).
136. Camacho, C. *et al.* BLAST plus : architecture and applications. *Bmc Bioinformatics* **10**, 421 (2009).
137. Altschul, S.F., Gish, W., Miller, W., Myers, E.W. & Lipman, D.J. Basic Local Alignment Search Tool. *Journal of Molecular Biology* **215**, 403-410 (1990).
138. Aramaki, T. *et al.* KofamKOALA: KEGG Ortholog assignment based on profile HMM and adaptive score threshold. *Bioinformatics* **36**, 2251-2252 (2020).
139. Jones, P. *et al.* InterProScan 5: genome-scale protein function classification. *Bioinformatics* **30**, 1236-1240 (2014).
140. Lohse, M. *et al.* Mercator: a fast and simple web server for genome scale functional annotation of plant sequence data. *Plant Cell and Environment* **37**, 1250-1258 (2014).
141. Kaul, S. *et al.* Analysis of the genome sequence of the flowering plant Arabidopsis thaliana. *Nature* **408**, 796-815 (2000).
142. Cheng, C.Y. *et al.* Araport11: a complete reannotation of the Arabidopsis thaliana reference genome. *Plant Journal* **89**, 789-804 (2017).
143. DOE-JGI. Brassica rapa FPsc v1.3. http://phytozome.jgi.doe.gov/ (2020).
144. Dohm, J.C. *et al.* The genome of the recently domesticated crop plant sugar beet (Beta vulgaris). *Nature* **505**, 546-+ (2014).
145. Jarvis, D.E. *et al.* The genome of Chenopodium quinoa. *Nature* **542**, 307-312 (2017).
146. Xu, C. *et al.* Draft genome of spinach and transcriptome diversity of 120 Spinacia accessions. **8**, 15275 (2017).
147. Schmutz, J. *et al.* Genome sequence of the palaeopolyploid soybean. *Nature* **463**, 178-183 (2010).
148. USDA-NIFA, D.-J.a. Phaseolus vulgaris v2.1. http://phytozome.jgi.doe.gov/ (2020).
149. Hosmani, P.S. *et al.* An improved de novo assembly and annotation of the tomato reference genome using single-molecule sequencing, Hi-C proximity ligation and optical maps. *bioRxiv*, 767764 (2019).
150. Barchi, L. *et al.* A chromosome-anchored eggplant genome sequence reveals key events in Solanaceae evolution. *Scientific Reports* **9**(2019).

bioRxiv preprint doi: https://doi.org/10.1101/2023.04.21.537482; this version posted April 23, 2023. The copyright holder for this preprint (which was not certified by peer review) is the author/funder, who has granted bioRxiv a license to display the preprint in perpetuity. It is made available under aCC-BY-NC-ND 4.0 International license.

151. McCormick, R.F. *et al.* The Sorghum bicolor reference genome: improved assembly, gene annotations, a transcriptome atlas, and signatures of genome organization. *Plant Journal* **93**, 338-354 (2018).
152. Maere, S., Heymans, K. & Kuiper, M. BiNGO: a Cytoscape plugin to assess overrepresentation of Gene Ontology categories in Biological Networks. *Bioinformatics* **21**, 3448-3449 (2005).
153. Shannon, P. *et al.* Cytoscape: A software environment for integrated models of biomolecular interaction networks. *Genome Research* **13**, 2498-2504 (2003).
154. Benjamini, Y. & Hochberg, Y. Controlling the False Discovery Rate - a Practical and Powerful Approach to Multiple Testing. *Journal of the Royal Statistical Society Series B-Methodological* **57**, 289-300 (1995).
155. Edgar, R.C. MUSCLE: multiple sequence alignment with high accuracy and high throughput. *Nucleic Acids Research* **32**, 1792-1797 (2004).
156. Castresana, J. Selection of conserved blocks from multiple alignments for their use in phylogenetic analysis. *Molecular Biology and Evolution* **17**, 540-552 (2000).
157. Darriba, D. *et al.* ModelTest-NG: A New and Scalable Tool for the Selection of DNA and Protein Evolutionary Models. *Molecular Biology and Evolution* **37**, 291-294 (2020).
158. Patro, R., Duggal, G., Love, M.I., Irizarry, R.A. & Kingsford, C. Salmon provides fast and bias-aware quantification of transcript expression. *Nat Methods* **14**, 417-419 (2017).
159. Love, M.I., Huber, W. & Anders, S. Moderated estimation of fold change and dispersion for RNA-seq data with DESeq2. *Genome Biology* **15**, 550 (2014).
160. Howe, E.A., Sinha, R., Schlauch, D. & Quackenbush, J. RNA-Seq analysis in MeV. *Bioinformatics* **27**, 3209-3210 (2011).
161. Bradford, M.M. A rapid and sensitive method for the quantitation of microgram quantities of protein utilizing the principle of protein-dye binding. *Anal Biochem* **72**, 248-54 (1976).
162. Perkins, D.N., Pappin, D.J.C., Creasy, D.M. & Cottrell, J.S. Probability-based protein identification by searching sequence databases using mass spectrometry data. *Electrophoresis* **20**, 3551-3567 (1999).
163. Searle, B.C. Scaffold: A bioinformatic tool for validating MS/MS-based proteomic studies. *PROTEOMICS* **10**, 1265-1269 (2010).
164. Usadel, B. *et al.* A guide to using MapMan to visualize and compare Omics data in plants: a case study in the crop species, Maize. *Plant Cell and Environment* **32**, 1211-1229 (2009).
165. Wan, S.B., Mak, M.W. & Kung, S.Y. mGOASVM: Multi-label protein subcellular localization based on gene ontology and support vector machines. *Bmc Bioinformatics* **13**(2012).
166. Daniel Gietz, R. & Woods, R.A. Transformation of yeast by lithium acetate/single-stranded carrier DNA/polyethylene glycol method. in *Methods in Enzymology*, Vol. 350 (eds. Guthrie, C. & Fink, G.R.) 87-96 (Academic Press, 2002).
167. Rodríguez-Navarro, A. & Ramos, J. Dual system for potassium transport in *Saccharomyces cerevisiae*. *Journal of Bacteriology* **159**, 940-945 (1984).
168. Schindelin, J. *et al.* Fiji: an open-source platform for biological-image analysis. *Nat Meth* **9**, 676-682 (2012).
169. Zhang, Y. *et al.* A highly efficient rice green tissue protoplast system for transient gene expression and studying light/chloroplast-related processes. *Plant Methods* **7**(2011).
170. Nelson, B.K., Cai, X. & Nebenfuhr, A. A multicolored set of in vivo organelle markers for co-localization studies in Arabidopsis and other plants. *Plant J* **51**(2007).
171. Studier, F.W. Protein production by auto-induction in high-density shaking cultures. *Protein Expression and Purification* **41**, 207-234 (2005).
172. Marley, J., Lu, M. & Bracken, C. A method for efficient isotopic labeling of recombinant proteins. *Journal of Biomolecular Nmr* **20**, 71-75 (2001).

bioRxiv preprint doi: https://doi.org/10.1101/2023.04.21.537482; this version posted April 23, 2023. The copyright holder for this preprint (which was not certified by peer review) is the author/funder, who has granted bioRxiv a license to display the preprint in perpetuity. It is made available under aCC-BY-NC-ND 4.0 International license.

173. Linding, R. *et al.* Protein disorder prediction: Implications for structural proteomics. *Structure* **11**, 1453-1459 (2003).
174. Lupas, A., Vandyke, M. & Stock, J. Predicting Coiled Coils from Protein Sequences. *Science* **252**, 1162-1164 (1991).
175. Wiedemann, C., Bellstedt, P. & Gorlach, M. CAPITO-a web server-based analysis and plotting tool for circular dichroism data. *Bioinformatics* **29**, 1750-1757 (2013).